

Miguel Cardoso Carreiró

Licenciado em Ciências da Engenharia Electrotécnica e de Computadores



Controlo de MPPT para Conversor DC-DC integrado alimentado por célula fotovoltaica

Dissertação para obtenção do Grau de Mestre em
Engenharia Electrotécnica e de Computadores

Orientador: Luís Augusto Bica Gomes de Oliveira, Prof. Auxiliar,
Universidade Nova de Lisboa.

Co-orientadores:

Júri:

Presidente: Doutor André Teixeira Bento
Damas Mora - FCT/UNL

Arguentes: Doutor Carlos Manuel Ferreira
Carvalho - ISEL/IPL

Vogais: Doutor Luís Augusto Bica
Gomes de Oliveira - FCT/UNL

Controlo MPPT para Conversor DC-DC integrado de uma célula fotovoltaica orgânica

Copyright © Miguel Cardoso Carreiró, Faculdade de Ciências e Tecnologia, Universidade NOVA de Lisboa.

A Faculdade de Ciências e Tecnologia e a Universidade NOVA de Lisboa têm o direito, perpétuo e sem limites geográficos, de arquivar e publicar esta dissertação através de exemplares impressos reproduzidos em papel ou de forma digital, ou por qualquer outro meio conhecido ou que venha a ser inventado, e de a divulgar através de repositórios científicos e de admitir a sua cópia e distribuição com objetivos educacionais ou de investigação, não comerciais, desde que seja dado crédito ao autor e editor.

À família que me apoiou.

ACKNOWLEDGEMENTS

In this paragraph, I would like to express great appreciation for the trust and help given to me by my adviser the professor Luís Oliveira. Moreover, I am grateful for the help and time given to me by those who were involved in previous similar projects.

Finally, is necessary acknowledge the importance of the Electrical and Computer Engineering department from the Faculty of Science and Technology, Nova University Lisbon for the resources and opportunities given to me.

ABSTRACT

In the present time, humans try to research ways to make life as easy and convenient as possible. Thus, there is a growing interest in making everyday devices as small and as lightweight as possible. Consequently, there has been an increase in portable electronic devices and IoT. With this type of innovations, an increase in small portable devices is expected, that look to make the human lifestyle as practical as possible.

Portable devices are generally low power equipment, this enables the possibility of powering these through renewable energy. Since most of the renewable energies have low power density, the most appealing resource is the solar energy, being that the power density of the photovoltaic energy stands out when compared to the others. Since the use of raw renewable energy is not suited to direct utilization a DC-DC converter is required to adapt and boost the voltage fed to the device. Finally, it is required a MPPT technique so that the PV cell can function at its peak efficiency, in order to maximize the low energy available. Therefore, this thesis proposes the analyse of two different MPPT methods (Perturb & Observe and Incremental Conductance) and in both performances.

The MPPT methods were tested with the PV cell subjected to different irradiations ($1000W/m^2$, $750W/m^2$ and $500W/m^2$, with $25^\circ C$) and temperatures ($35^\circ C$, $25^\circ C$ and $15^\circ C$, with $1000W/m^2$).

The system with the Perturb & Observe technique obtained an efficiency of 99.39% with $1000W/m^2$, 99.97% with $750W/m^2$ and 75.11% with $500W/m^2$, while maintaining an efficiency above 99.30% with the different temperatures. Finally, using the Incremental Conductance technique obtained an efficiency of 99.57% with $1000W/m^2$, 88.08% with $750W/m^2$ and 62.88% with $500W/m^2$, while maintaining an efficiency above 99.04% with the different temperatures. The results demonstrate that both methods used are suitable to implement with harvesting systems of portable devices.

Keywords: Maximum Power Point Tracking, Maximum Power Point, Photovoltaic cells, Boost DC-DC converter.

RESUMO

Atualmente, a humanidade tenta procurar maneiras de fazer com que o dia a dia seja o mais fácil e conveniente possível. Deste modo, existe interesse em fazer com que os dispositivos utilizados diariamente se tornem o mais leve e pequeno possível. Consequentemente, esta procura faz com que tenha havido um grande aumento de dispositivos eletrônicos portáteis e IoT. Assim sendo, o aumento da utilização de dispositivos eletrônicos portáteis é previsto, de modo a que o estilo de vida humano se torne o mais facilitado possível.

Dispositivos elétricos portáteis por norma são equipamentos de baixa potência, possibilitando que estes sejam alimentados através de energias renováveis. Visto que a maior parte das energias renováveis apresenta baixa densidade de potência, a fonte renovável mais atrativa é a energia solar, visto que esta apresenta a maior densidade de energia quando comparada a outras. Dado que, a energia recolhida por fontes renováveis não é adequada para utilização direta, a aplicação de um conversor DC-DC é necessária de modo a adaptar e levantar a tensão recebida para alimentação de um dispositivo eletrónico. Finalmente, será necessária uma técnica MPPT de modo a que a célula fotovoltaica possa funcionar com máximo de eficiência, de modo a que seja maximizada a energia disponível. Deste modo, esta tese propõe a análise de dois diferentes métodos MPPT (Perturbar & Observar e Condutância Incremental) e suas performances.

Os métodos MPPT foram testados com uma célula fotovoltaica subjugada a diferentes valores de irradiação ($1000W/m^2$, $750W/m^2$ e $500W/m^2$, a $25^\circ C$) e temperatura ($35^\circ C$, $25^\circ C$ e $15^\circ C$, a $1000W/m^2$).

O sistema com o método Perturbar & Observar obteve uma eficiência de 99.39% a $1000W/m^2$, 99.97% a $750W/m^2$ e 75.11% a $500W/m^2$, mantendo sempre uma eficiência superior a 99.30% com as diferentes alterações de temperatura. Finalmente, usando o método de Condutância Incremental obtiveram-se eficiências de 99.57% a $1000W/m^2$, 88.08% a $750W/m^2$ e 62.88% a $500W/m^2$, mantendo sempre uma eficiência superior a 99.04% com as diferentes alterações de temperatura. Os resultados demonstram que ambos os métodos são adequados para implementação com sistemas de recolha de dispositivos portáteis.

Palavras Chave: Localização de Pontos de Potência Máxima, Pontos de Potência Máxima, Células Fotovoltaicas, Conversor Boost DC-DC.

CONTENTS

Conteúdo

1	INTRODUCTION	1
1.1	Motivation and context	1
1.2	Specifications	2
1.3	Organization	2
1.4	Main Contributions	3
2	STATE OF THE ART.....	5
2.1	Basic Voltage Converters	5
2.1.1	Linear converters	6
2.1.2	Switched converters	7
2.2	Maximum Power Point Tracking Techniques	14
2.2.1	Hill Climbing/ Perturb & Observe (P&O)	14
2.2.2	Incremental Conductance (IncCond)	16
2.2.3	Fractional Open-Circuit Voltage	17
2.2.4	Fractional Short-Circuit Current	18
2.2.5	Fuzzy Logic Control	19
2.2.6	Neural Network	19
2.2.7	Ripple Correlation Control (RCC)	19
2.2.8	Current Sweep	20
2.2.9	DC-Link capacitor Droop Control	21

2.2.10	Load Current or Load Voltage Maximization.....	22
2.2.11	dP/dV or dP/dI Feedback Control	22
2.3	Comparison of MPPT methods.....	23
3	PROPOSED SYSTEMS.....	26
3.1	PV array	27
3.2	DC-DC boost Converter.....	30
3.3	Max power point tracking method	31
3.3.1	<i>Perturb and observe</i>	32
3.3.2	<i>Incremental Conductance Max power point tracking method</i>	33
4	SIMULATIONS AND RESULTS	35
4.1	Simulations of the DC-DC Converters.....	37
4.1.1	<i>Without a MPPT technique</i>	37
4.1.2	<i>With P&O</i>	40
4.1.3	<i>With Incremental Conductance</i>	43
4.2	Discussion	45
5	CONCLUSIONS AND FUTURE WORK	47
5.1	Conclusions.....	47
5.2	Future Work	48
6	BIBLIOGRAPHY	49

LIST OF FIGURES

Figure 1.1 - Block diagram of the proposed system	2
Figure 2.1 - Linear series converter.....	6
Figure 2.2 - Linear shunt converter.....	7
Figure 2.3 - Basic Boost DC-DC converter circuit	9
Figure 2.4 - Basic Boost DC-DC converter circuit, when S1 closed	10
Figure 2.5 - Basic Boost DC-DC converter circuit, when S1 opened.....	10
Figure 2.6 - Voltage in L , <i>in function of time</i>	10
Figure 2.7 - Power Voltage/Current Curve from PV cell	14
Figure 2.8 - P&O/Hill climbing under changing atmospheric conditions ...	15
Figure 2.9 - P&O algorithm	16
Figure 2.10 - IncCond algorithm.....	17
Figure 2.11 - Topology of a DC-Link Capacitor Droop Control.....	22
Figure 3.1 - Proposed MPPT algorithm for PV application	26
Figure 3.2 - PV cell IV and PV curves.....	27
Figure 3.3 - Effect of different values of irradiance in a PV cell at 25°C	28
Figure 3.4 - Effect of Temperature variations in a PV cell at 1KW/m ²	29
Figure 3.5 - Simulink model of DC-DC boost converter	30
Figure 3.6 - Pulses and voltage of the switch and inductor current.....	31
Figure 3.7 - MPPT PV cell powered system	32
Figure 3.8 - Model of P&O.....	32
Figure 3.9 - Model of IncCond.....	33

Figure 4.1 - Irradiance and Temperature changes in the simulations.....	36
Figure 4.2 - System without MPPT technique.....	37
Figure 4.3 - PV cell Power without MPPT	38
Figure 4.4 - PV cell voltage and DC-DC output voltage	38
Figure 4.5 - PV cell Power with P&O MPPT	40
Figure 4.6 - PV cell voltage and DC-DC output voltage with P&O.....	41
Figure 4.7 - PV cell Power with IncCond MPPT	43
Figure 4.8 - PV cell voltage and DC-DC output voltage with IncC.....	44

LIST OF TABLES

Table 2.1 - Principle of functioning of MPPT Hill Climbing/P&O	15
Table 2.2 - Characteristics of various MPPT Technique.....	24
Table 3.1 - PV cell parameters	27
Table 3.2 - Converter sizing *instead of the calculated 151uH the 150uH can be found in the market	30
Table 4.1 - MPP of the PV cell with varying the irradiance	36
Table 4.2 - MPP of the PV cell with varying the temperatures	37
Table 4.3 - Circuit with no MPPT with varying the irradiance	39
Table 4.4 - Circuit with no MPPT with varying temperature.....	39
Table 4.5 - Circuit with P&O with varying irradiance	41
Table 4.6 - Circuit with P&O with varying temperature	42
Table 4.7 - Circuit with IncCond with varying irradiance	44
Table 4.8 - Circuit with IncCond with varying temperature	45

ACRONYMS

DC-DC-Direct Current to Direct Current

DSP - Digital Signal Processor

IncCond - Incremental Conductance

MPP - Maximum power Point

MPPT- Maximum power Point Tracking

PMU - Power Management Unit

P&O - Perturb & Observe

PV - Photovoltaic

PWM - Pulse Width Modulation

RCC - Ripple Correlation Control

CHAPTER 1

INTRODUCTION

1.1 Motivation and context

With the introduction of the 21st century there has been an increase in the daily use of electronic devices that make possible the improvement of the human life, consequently the average person owns around six of these devices [1], such as smartphones, tablets, smart watches and computers.

Therefore, there is interest in methods that allow the operation of the portable electronic devices without the need of connection to the power grid, neither the regular replacement of batteries, making the use of renewable energy appealing.

As the interest of the harvest of renewable energy is at its peak, there has been the development of various sources to gather it [2], such as photovoltaic [3], thermoelectric [4], piezoelectric [5] and electromagnetic energy [6].

Despite the great abundance of procedures to harvest renewable energy these kinds of methods generally feature low energy density. Therefore, generally if one is used it is required the use of a Power Management Unit to provide as a constant voltage source, making the system capable of self-sustainability. This PMU will use a DC-DC converter, allowing a step up of the voltage received from the energy harvesting method.

Furthermore, since the energy available to the system is generally low it is essential that the harvesting method can perform at its MPP, therefore a Maximum power Point Tracking method (MPPT) is generally implemented to boost up efficiency.

By combining the previous technologies, it is possible to create a system capable of feeding a low power device through renewable energy.

1.2 Specifications

This project aims to find among the different techniques an adequate MPPT method capable to be integrated in a system similar to the previously mentioned, therefore the MPPT technique must be able to operate with low power as well as be sensitive enough to adapt to the environment in which the PV cell will operate maintaining the harvesting procedure near MPP.

Hence, It is proposed a system that harvests energy through a small photovoltaic panel, the voltage will be then increased by a boost DC-DC, where finally a MPPT technique will serve to control the system maintaining it with high efficiency. The simplified block diagram of the system can be seen in the Figure 1.1.

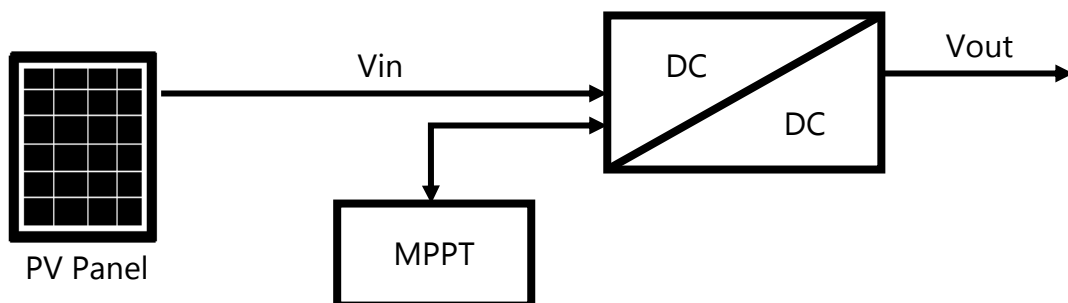


Figure 1.1 - Block diagram of the proposed system

1.3 Organization

This dissertation is organized in five chapters. The first chapter explains the motivation and specifications for the two proposed MPPT methods. In the second chapter, the different types of basic DC-DC converters and different MPPT techniques are analysed and studied. In the third chapter, the specifications and performance of the PV cell and the boost DC-DC used are exhibited, furthermore the two MPPT techniques models are conveyed. In the fourth, are represented the result of both MPPT models, furthermore a model where no MPPT technique is used so that comparison can be provided for the developed systems. In the last one, the conclusions are shown and future perspective for the models are proposed.

1.4 Main Contributions

This work aims to look into two different MPPT methods able to function with a boost DC-DC in a low power system. Its components, such as the PV cell, DC-DC converters and MPPT methods used to simulate the system are developed and explained. The main contributions of this work, are:

- The research into the properties that make the use of MPPT methods advantageous as well as their drawback, the properties required to a MPPT technique when paired with a low power system, and the development of the methods Perturb & Observe and Incremental Conductance.
- The Perturb & Observe technique implemented with a PV cell and a boost DC-DC with efficiencies from 99.97% to 75.11%.
- The Incremental Conductance technique implemented with a PV cell and a boost DC-DC with efficiencies from 99.91% to 62.88%.
- Model controlled by direct duty cycle with a PV cell and a boost DC-DC with efficiencies from 99.91% to 55.19%.
- A result comparison between the proposed Methods (Power, maximum voltage output, efficiency, etc.).

CHAPTER 2

STATE OF THE ART

As previously mentioned, the energy to be used in this project is provided by the ambient, and generally this kind of raw energy is not suitable to power electronic circuits, meaning there is a need to stabilize, increase (boost operation) or decrease (buck operation) the voltage to meet the requirements of the circuit powered by it.

Since the energy available in the process is rather low there is a necessity in achieving the maximum efficiency possible, therefore the implementation of a MPPT controller is desirable.

In this chapter different types of basic DC-DC converters and MPPT controllers will be reviewed, analysing their main proprieties.

2.1 Basic Voltage Converters

As the name implies a voltage converter will have the task of transforming a voltage into another, this ability makes the pairing with renewable energy harvesting technology a good combination, as it has the ability to stabilize and adapt the energy received, protecting the devices from overload voltages by decreasing or increasing the voltage to the needs of the device in use. In the case of this work, a PV based system, pairing a voltage converter with a MPPT algorithm will enable the PV cell to achieve the optimal power operation [34].

This usefulness has pushed the development of several types of voltage converters, that can be distinguished in two different categories, linear converters and switched converters.

This project uses a switched inductive boost DC-DC converter, since a single inductor can be used in a voltage converter to obtain a desirable voltage without loss in efficiency and without the need to several phases, as can be seen in this chapter.

2.1.1 Linear converters

Linear voltage converters are the simplest types of converter, being its only purpose to decrease the input voltage to a set output voltage that is kept constant by a controller circuit.

This kind of converter can be implemented in a shunt or series topology, where the surplus of energy is dissipated by a load.

As implied by the name, in the series topology the regulator load is connected in series, between the input and the load. The converter will act as if it was a variable resistor R_s , modifying the voltage V_{in} into a desired V_{out} . When the load R_L shows variations the controller circuit readjusts its resistance value (R_s), so that V_{out} is kept to a constant value. The value of V_{out} is a predetermined value so that the controller circuit can readjust R_s .

Since linear converters only decrease the input voltage, it will naturally achieve a higher efficiency the smaller the difference of the input and output voltages, as the value is the ratio between these voltages (V_{out}/V_{in}).

This kind of converter is shown in the Figure 2.1.

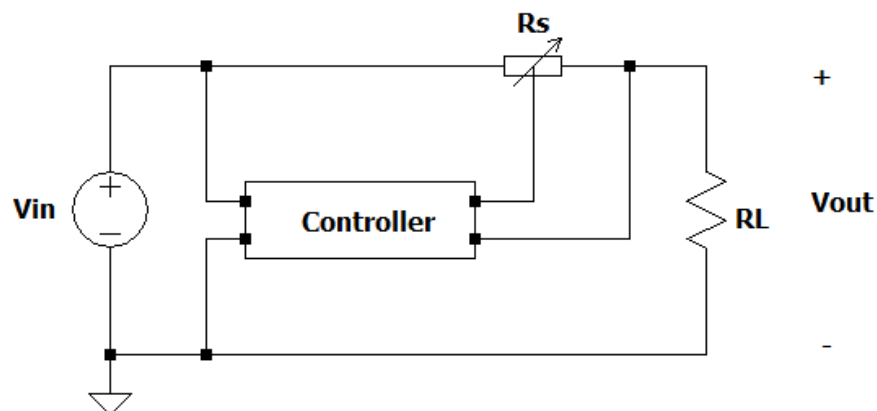


Figure 2.1 - Linear series converter

In the shunt method there is a regulator load that is placed in parallel with the load. In this method there is a necessity of a resistor R_{in} between the input voltage and the regulator load as represented by the Figure 2.2. This resistor can be either the output resistance of the source supplying, an added resistor or the combination of both.

As the previous topology, the controller circuit will allow constant output voltages, while load variations might occur, by adjustment of the value from the regulator load R_s .

Shunt converters efficiency is not ideally independent of the output Power as the series converters, the way of achieving maximum performance happens when the maximum output Power is achieved.

Linear converters are quite simple, making them very appealing. Nevertheless, when pairing a PV cell with a converter it's required of the converter the elevation of the voltage that receives. Consequently, linear converters are not suited for this kind of project, since these can only decrease the energy received. In addition, the losses typically verified in these converters make them unsuited, due the limited energy provided by a PV cell.

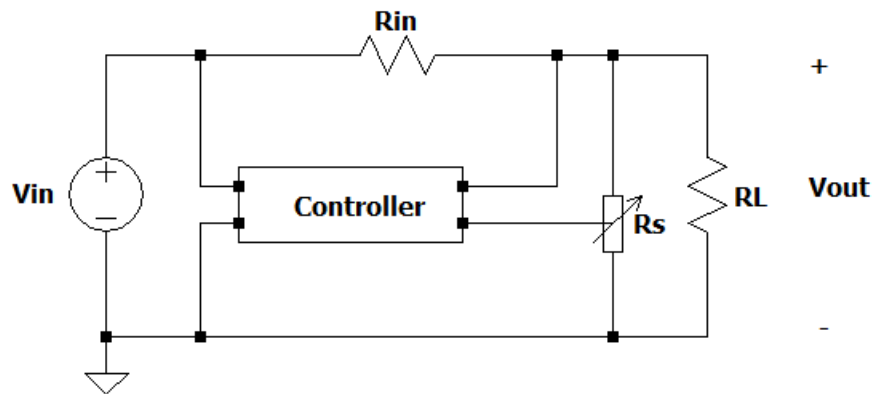


Figure 2.2 - Linear shunt converter

2.1.2 Switched converters

Switched converters, unlike linear converters are theoretically lossless since no resistors are used. Instead, the process of transforming a DC voltage into another DC voltage value relies on the transference of energy from the input into a reactive element (an inductor or a capacitor) and then retrieving that energy to the output, in order to achieve a desired output voltage. Although, there are differences between the use of an inductor or capacitor, as the voltage in a capacitor cannot have discontinuities and the voltage across an inductor is able to change abruptly and have discontinuity. The ability to change voltage abruptly, enables that a larger voltage in the output than the in input can be achieved when an inductor is used, in contrast a single capacitor can only lower the input voltage.

While using inductor or capacitors is important to have in consideration the efficiency of energy being transferred. When using these components in a DC-DC converter, these elements are connected to a voltage source (V_{in}) through switches, and these switches have ON resistances (R_{sw}).

When charging a capacitor, the voltage will increase until it reaches V_{in} while the inductor charges until it reaches a current of V_{in}/R_{sw} . The voltage in a capacitor can be calculated through

$$v_c(t) = V_{in} \left(1 - e^{-\frac{t}{RC}} \right) \quad (2.1)$$

and the current in the inductor by

$$i_l(t) = \frac{V_{in}}{R} \left(1 - e^{-\frac{Rt}{L}} \right) \quad (2.2)$$

When the capacitor is being charged, almost all the energy from the source voltage is dissipated in the resistor (R_{sw}). When the capacitor is fully charged, the energy dissipated through the resistor will equal the energy stored in the capacitor during the charging process. Meaning that the max efficiency of charging is 50%, meaning that when capacitors are used in voltage converter these should be always fully charged to guarantee max efficiency. Output voltages greater than the source voltage can be achieved using capacitors, but various capacitors are necessary with multiple phases. In a first phase, a capacitor is connected parallel with the source voltage, and during a second phase the capacitors are arranged in series enabling a larger output voltage. The efficiency of voltage converters using capacitors can be boosted if the number of capacitors is close to the necessary voltage ratio between the source and output voltages.

In contrast, when an inductor is charged almost all the energy of the source is transferred to the inductor. As a result, efficiency will drop as the inductor is charged to its maximum current. Consequently, to maximize efficiency, the voltage converter will benefit if the switches prevent the full charge of the inductor. In contrast with the use of capacitors a single inductor can be used in a voltage converter to obtain a desirable voltage without loss in efficiency.

Voltage regulation in switched voltage converters cannot be neglected as it has the function of powering electronic circuits, as such the load requires a regulated output voltage to operate. This regulation will be obtained by a control system that manages the switch to be ON or OFF by acting as the duty cycle of the switch maintaining the frequency stabilized while lowering or boosting the output voltage as required.

2.1.2.1 Inductive boost DC-DC converter

Using an inductor to charge a capacitor, instead of the source voltage may benefit the efficiency of the circuit. This is the basic concept of a step-up converter. Fig. 2.3 represents the basic

structure of the boost DC-DC converter. Regarding the capacitor C has the function to attenuate the ripple from the output voltage.

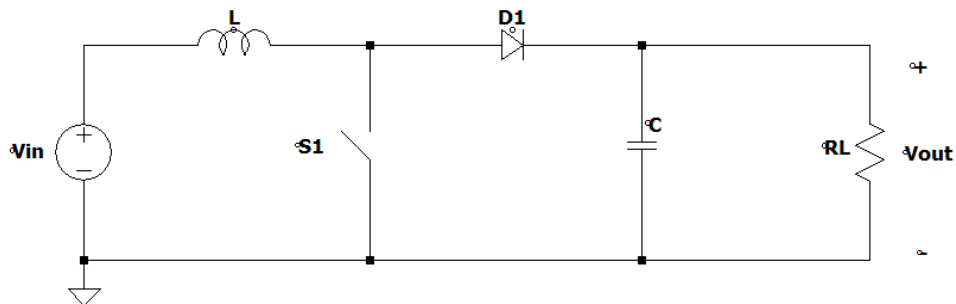


Figure 2.3 - Basic Boost DC-DC converter circuit

The functioning of this converter begins when S_1 is in its closed position, Figure 2.4. During that period the Inductor L begins to charge. As for the current through the inductor linearly increases until the S_1 opens, or saturation is achieved. When the switch opens, Figure 2.5, the current stored in the inductor is forced to the output.

As previously mentioned, controlling the ratio that S_1 is ON and OFF, the duty cycle (δ), allows control over the current stored in L . With this, a δ can be chosen to prevent the full discharge, this way the current received by the load will be always superior to the previous cycle until saturation is reached.

This kind of basic boost DC-DC converter can operate in two modes, the current continuous mode (CCM) and the current discontinuous mode (CDM). The converter operates in CCM if the current through the inductor never reaches zero, meaning the switch will be closed during a larger time interval than open. Another also relevant factor, so that the inductor never fully discharges, is the inductance itself.

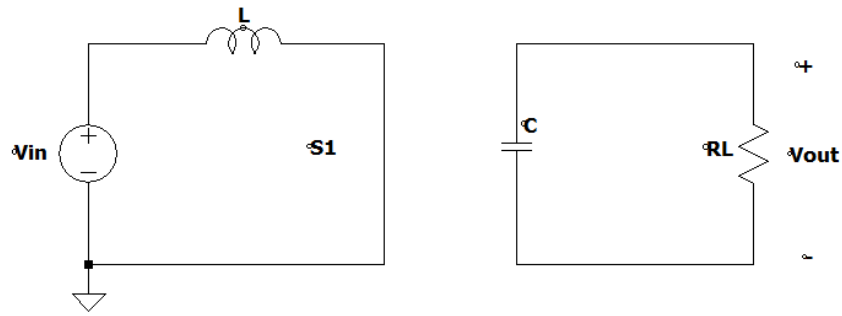


Figure 2.4 - Basic Boost DC-DC converter circuit, when S_1 closed

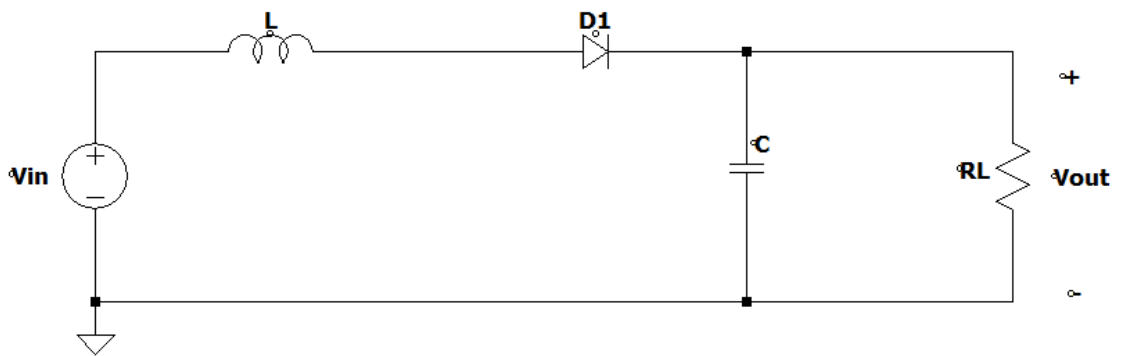


Figure 2.5 - Basic Boost DC-DC converter circuit, when S_1 opened

Assuming that the circuit is operating in ideal conditions, the energy change in L in a whole period, is zero. Being that the voltage in L (v_L) is v_{in} while S_1 is closed (T_1) and ($v_{in} - v_{out}$) when S_1 is open (T_2), as shown in Fig.2.6.

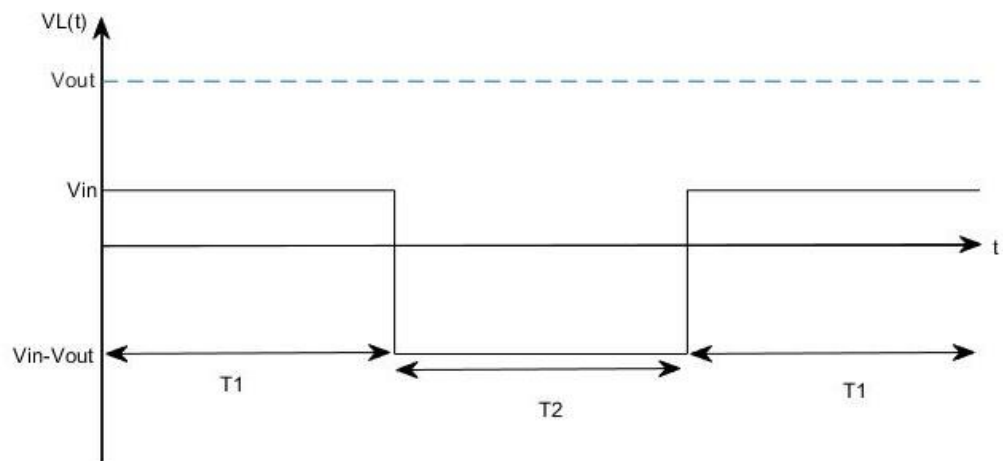


Figure 2.6 - Voltage in L , in function of time

Thus, the voltage in v_L during a period T_{clk} can be obtain through

$$\int_0^{T_{clk}} v_L(t) dt = v_{in}T_1 + (V_{in} - V_{out})T_2 = 0 \quad (2.3)$$

By rearranging (2.3), assuming that the duty cycle is given by $T_1/(T_1 + T_2)$, the ratio between output and input is

$$\frac{v_{out}}{v_{in}} = \frac{T_1 + T_2}{T_2} = \frac{1}{1 - \delta} \quad (2.4)$$

As shown in (2.4) the ratio between output and input can be adjusted by controlling the duty-cycle (δ).

Since the period is given by $(T_1 + T_2)$, the frequency of operation can be given by (2.5)

$$F_{clk} = \frac{V_{out} - V_{in}}{V_{out}T_1} = \frac{V_{in}}{V_{out}T_2} \quad (2.5)$$

As previously mentioned, the current present in the inductor is variable during the opening and closing of the switch. As such, the current present in the inductor can be obtained by adding its average value (I_L) with the ripple from v_L , therefore

$$i_L(t) = I_L + \Delta i_L(t) \quad (2.6)$$

The I_L ripple can be obtained through the voltage that goes through the inductor where

$$\begin{aligned}\Delta i_L &= \frac{1}{L} \int_0^{T_{clk}} v_L(t) dt = \frac{v_{in}T_1}{L} = \frac{(V_{in} - V_{out})T_2}{L} = \frac{v_{in}T\delta}{L} \\ &= \frac{(V_{in} - V_{out})T(1 - \delta)}{L}\end{aligned}\tag{2.7}$$

Using (2.5) it is possible to ascertain the inductor value as shown in (2.8)

$$L = \frac{V_{in}\delta}{\Delta i_L \cdot F_{clk}} = \frac{(V_{in} - V_{out})(1 - \delta)}{\Delta i_L \cdot F_{clk}}\tag{2.8}$$

If no losses happen in the system, it can be assumed that the power in the input will be equal to the output. This way is possible to achieve the current in the input (I_{in}) using (2.9), it also known that $I_{out} = \frac{V_{out}}{R_{out}}$

$$I_{in} = I_L = \frac{V_{out}}{V_{in}} I_{out} = \frac{1}{1 - \delta} \frac{V_{out}}{R_{out}}\tag{2.9}$$

Regarding the capacitor, in a steady state the average current will be zero. As result, the average current in the output will be the current that passes through the diode i_D . Furthermore, the current ripple in the diode will be filtered by the capacitor

$$i_C(t) \cong \Delta i_D(t) = i_D - I_{out}\tag{2.10}$$

As the value for the capacitor, since the current in it can be given by $I_c = C \cdot dV/dt$, its value can be given by (2.11)

$$C \frac{dV_{out}}{dt} = -C \frac{\Delta V_{out} F_{clk}}{\delta} = -\frac{V_{out}}{R_{out}} \quad (2.11)$$

$$C = \frac{V_{out} \delta}{\Delta V_{out} R_{out} F_{clk}} = \frac{V_{in} \delta}{\Delta V_{out} (1 - \delta) R_{out} F_{clk}}$$

At last, the efficiency of the converter is given by the ratio between the power given to the load (P_{out}) and the power given to the converter (P_{in}). Since the power given is dissipated through the converter it will create a power loss (P_{loss}), as explicit in (2.12).

$$\eta = \frac{P_{out}}{P_{in}} = \frac{P_{out}}{P_{out} + P_{loss}} \quad (2.12)$$

2.2 Maximum Power Point Tracking Techniques

As previously mentioned, there is the objective of powering a low power circuit with a PV cell. Thus, the tracking of the MPP of the PV cell is usually essential [7]. Therefore, a lot of MPPT methods have been developed, that vary largely from one another.

As shown in Fig. 2.7, there is interest in maintaining the system functioning in the region of V_{MPP} or I_{MPP} , making the PV system operating in its maximum power point. As for choosing one MPPT method will depend on the properties of the system and where it will be implemented, since each implementation will face different types of hurdles, from low energy availability, complexity, costs, sensors needed, convergence speed required and possible multiple local maximus.

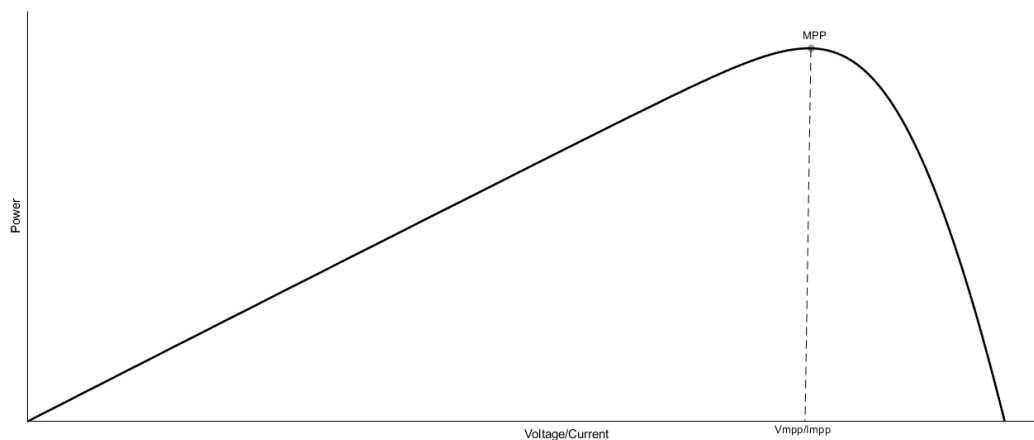


Figure 2.7 - Power Voltage/Current Curve from PV cell

2.2.1 Hill Climbing/ Perturb & Observe (P&O)

Hill Climbing [8]-[11] is a method that will create a perturbation in the duty ratio of the power converter, and P&O [11]-[13] in the operation voltage of the PV. When a PV array is connected to a power converter, a perturbation in the duty ratio of the converter will modify the current of the PV and consequently its voltage.

As shown in Figure 2.7 on the left of the MPP the increase of the voltage/current will bring the power closer to its max power point, as well as decreasing the voltage/current on the right side. This understanding is the operation base of this method, its functioning method can be easily represented by the Table 2.1 and Figure 2.9, this process is repeated periodically until the MPP is reached. The perturbation size can be adjusted to reduce the oscillations but consequently it will slow down the MPPT.

These two methods can fail to effectively achieve the MPP in conditions where there are changes in atmospheric conditions, this can be demonstrated by Fig.2.8. in tracking of the MPP

the method is in the position A as shown in Fig.2.8, a perturbation dV occurs at the same time the atmospheric conditions change and instead of the power registered in the position B now it obtains the power in the position C, since this power is greater than in A the next perturbation will be a positive moving away the system from the MPP.

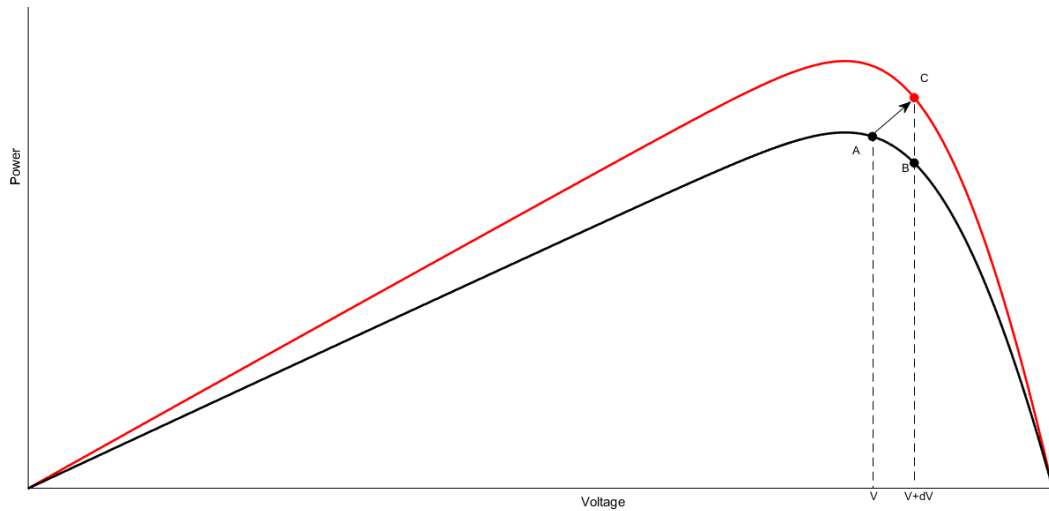


Figure 2.8 - P&O/Hill climbing under changing atmospheric conditions

Perturbation	Change in Power	Next Perturbation
Positive	Positive	Positive
Positive	Negative	Negative
Negative	Positive	Negative
Negative	Negative	Positive

Table 2.1 - Principle of functioning of MPPT Hill Climbing/P&O

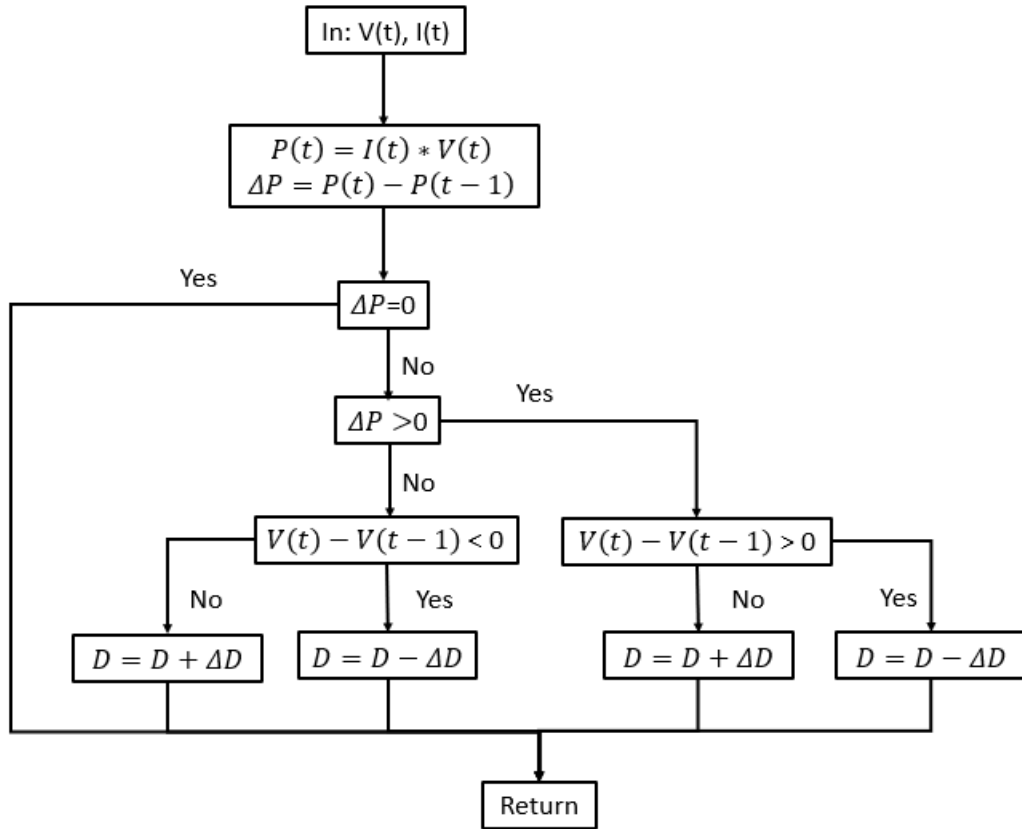


Figure 2.9 - P&O algorithm

2.2.2 Incremental Conductance (IncCond)

The Incremental conductance [11] [14]-[17], method takes base on the fact that the slope of the PV array Power Voltage graph (Fig 2.7) is zero at the MPP, positive on its left and negative on its right.

$$\begin{cases} dP/dV = 0 , \text{ at MPP} \\ dP/dV > 0 , \text{ left of MPP} \\ dP/dV < 0 , \text{ right of MPP} \end{cases}$$

(2.11)

Being that,

$$\frac{dP}{dV} = \frac{d(IV)}{dV} = I + V \frac{dI}{dV} \approx I + V \frac{\Delta I}{\Delta V}$$

(2.12)

(2.12) can be rewritten as

$$\begin{cases} \Delta I/\Delta V = -I/V , \text{ at MPP} \\ \Delta I/\Delta V > -I/V , \text{ left of MPP} \\ \Delta I/\Delta V < -I/V , \text{ right of MPP} \end{cases}$$

(2.13)

With such knowledge an algorithm as shown in Fig.2.10 can be used to implement this MPPT method, V_{ref} in this case will be the voltage at which the PV is operating. As shown the method will decrement or increment V_{ref} to track the MPP, once this point is reached it will be maintained, unless changes in the system cause a shift in the MPP.

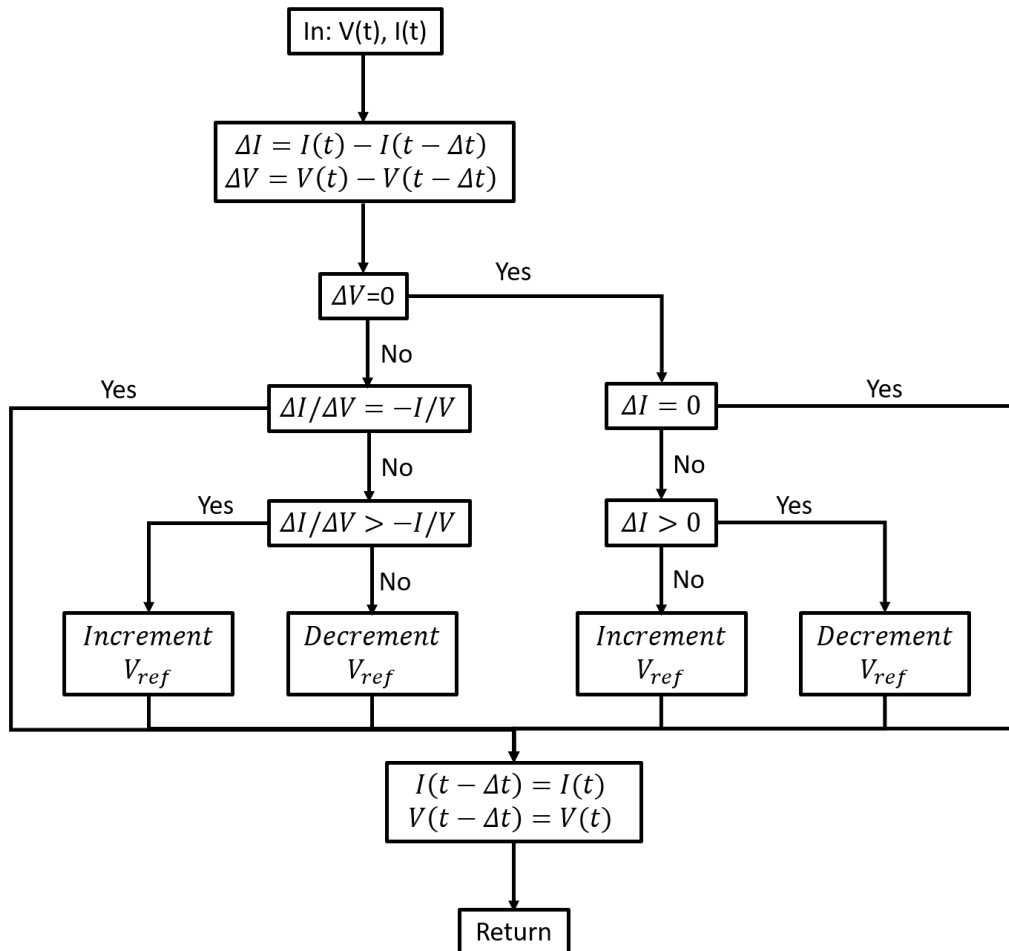


Figure 2.10 - IncCond algorithm

Once again, as the previous methods the increment size can be adjusted. If it is required a fast tracking, a bigger increment can be used but the system might not operate in the MPP but oscillate about it instead, as such, the system requirements must be considered.

2.2.3 Fractional Open-Circuit Voltage

Fractional open-circuit voltage method [11][18]-[20], is based on the almost linear relationship between V_{MPP} and V_{OC} (2.14) of the PV array, under different temperatures and irradiance indices.

$$V_{MPP} \approx k_1 V_{OC} \quad (2.14)$$

The proportionality of V_{MPP} and V_{OC} will be given by the constant k_1 . This constant k_1 will be dependent on the PV array used, and it is usually computed by empirically determining V_{MPP} and V_{OC} of the array at different temperatures and Irradiances. This factor has been usually reported in values between 0.71 and 0.78.

Once the value of k_1 is known, V_{MPP} is obtain through (2.14), where the value of V_{OC} is obtained by periodically shutting down the power of the converter. As expected, the shutting down of the converter implicates some disadvantages, as the temporary loss of power. To prevent these impracticalities, pilot cells with characteristics similar to the PV array in use can be used.

Since as previously mentioned, this method will only use the almost linear relationship between V_{MPP} and V_{OC} , meaning that technically the system will never operate in the true value of the MPP. Even so, the cheap and easy implementation makes this MPPT method desirable for some implementations.

2.2.4 Fractional Short-Circuit Current

In similarity with Fractional open-circuit voltage, the Fractional Short-Circuit Current method [11][20]-[22] will be based on the approximately linearly relation between PV array parameters, this time the currents as shown in (2.15)

$$I_{MPP} \approx k_2 I_{SC} \quad (2.15)$$

As in the previous k_2 will be a proportionality constant, that must be pre-determined according the characteristics of the PV array in use. This constant is as a rule between the values 0.78 and 0.92.

Obtaining the value of I_{SC} during the running of the circuit is quite problematic, due to the need for a short circuit. An additional switch is needed so that the circuit can be shorted periodically, so that I_{SC} is obtainable, this way there is an increasing in the number of components and cost.

2.2.5 Fuzzy Logic Control

With the possible implementation of microcontrollers in MPPT methods made the use of Fuzzy Logic Control [11][23]-[25] raise in popularity.

The Fuzzy logic control is based in three different states: fuzzification, the check of the rules table, and defuzzification. The controller will find the operation zone and adjust it by varying the duty cycle.

This kind of MPPT has advantages of working with imprecise inputs, the ability to handle nonlinearity as well as not needing an accurate mathematical model.

2.2.6 Neural Network

As well as the previous method, the Neural Network [11][26][27] method is quite well adapted for microcontrollers.

Neural networks usually are composed by three layers: Input, hidden and output layer. These layers are composed by nodes and can vary in its number according to the user. Generally, for PV arrays the input nodes are a combination of parameters like V_{OC} and I_{SC} and atmospheric data. The output is generally the duty cycle that will operate the power converter in MPP.

The accuracy of the Neural Network will depend on how well it was trained.

This kind of method has the disadvantage of the need to be specifically trained to a kind of PV array, since different types of PV will have different characteristics, as well the need to be periodically trained to guarantee accurate MPPT.

2.2.7 Ripple Correlation Control (RCC)

In a PV array connected to a power converter, the switching action of the power converter imposes voltage and current ripple on the PV array. As such, the PV array power is also subjected to ripple. With this the RCC [11][28] method, uses the ripple to perform MPPT. RCC method will correlate the time derivative of the time-varying PV array power (\dot{p}) with the time derivative of the time-varying PV array current of voltage (i or v) to drive the power gradient to zero.

As shown in Fig.2.8, when the derivative of the power is zero the MPP is reached, as such if the current or voltage are increased and power is increasing as well, then the operating point is on the left the MPP ($\dot{p} > 0, \dot{v} > 0, \dot{i} > 0$). On the contrary, if there is an increase in the voltage or current and the power is decreasing ($\dot{p} < 0$) then the MPP the operating point has passed the MPP and is operating on its right. Using such facts, it can be obtained that $\dot{p}\dot{v}$ or $\dot{p}\dot{i}$ are positive on the left of the MPP, negative on the right of MPP and zero in the MPP.

2.2.8 Current Sweep

As implied by the name, the current sweep method [11][29] will sweep the waveform from the PV array current until the I-V characteristic of the PV array is obtained, this procedure will be updated in fixed interval times. Then the V_{MPP} can be obtained through the I-V characteristic curve.

For the sweep waveform it is chosen a directly proportional derivative as represented in (2.16) where k_4 is a proportionality constant

$$f(t) = k_4 \frac{df(t)}{dt} \quad (2.16)$$

The PV array power is given by

$$p(t) = v(t)i(t) = v(t)f(t) \quad (2.17)$$

Since the derivative of the power is zero in the MPP, we have

$$\frac{dp(t)}{dt} = v(t) \frac{df(t)}{dt} + f(t) \frac{dv(t)}{dt} = 0 \quad (2.18)$$

Using (2.16) in (2.18) gives

$$\frac{dp(t)}{dt} = \left[v(t) + k_4 \frac{dv(t)}{dt} \right] \frac{df(t)}{dt} \quad (2.19)$$

The solution of equation (2.16) has the solution of

$$f(t) = C \exp [t/k_4]$$

(2.20)

Where C is chosen to be equal to the maximum PV array current I_{max} , this current can be obtained by using current discharges through the capacitor, and k_4 negative, so that (2.20) is a decreasing exponential function with time constant $\tau = k_4$. As so its derivate will be a nonzero, (2.19) can be divided by $df(t)/dt$ will be the simplified to

$$\frac{dp(t)}{df(t)} = v(t) + k_4 \frac{dv(t)}{dt} \quad (2.21)$$

Since $f(t) = i(t)$ (2.21) it's obtained

$$\frac{dp(t)}{di(t)} = v(t) + k_4 \frac{dv(t)}{dt} \quad (2.22)$$

Once the V_{MPP} is obtained after using the current sweep, its value can be double checked using equation (2.22).

2.2.9 DC-Link capacitor Droop Control

DC-Link capacitor Droop Control [11][30] is MPPT technique specially designed to be connected in parallel with an AC system.

In this method the duty cycle is given by

$$d = 1 - \frac{V}{V_{link}} \quad (2.23)$$

In this case V is voltage given by the PV array and V_{link} is the voltage across the dc link, as can be seen in Fig. 2.11. Case V_{link} is kept constant and the current going to the inverter is increased, the power in the boost converter will increase and consequently increase the power coming from the PV array. While this current is increased, V_{link} can be kept constant seeing that the power required by the inverter does not surpass the available power. When the

power available is surpassed the V_{link} drops, being that right before this point the current of the inverter is at its maximum point, meaning that the PV array is operating in its MPP.

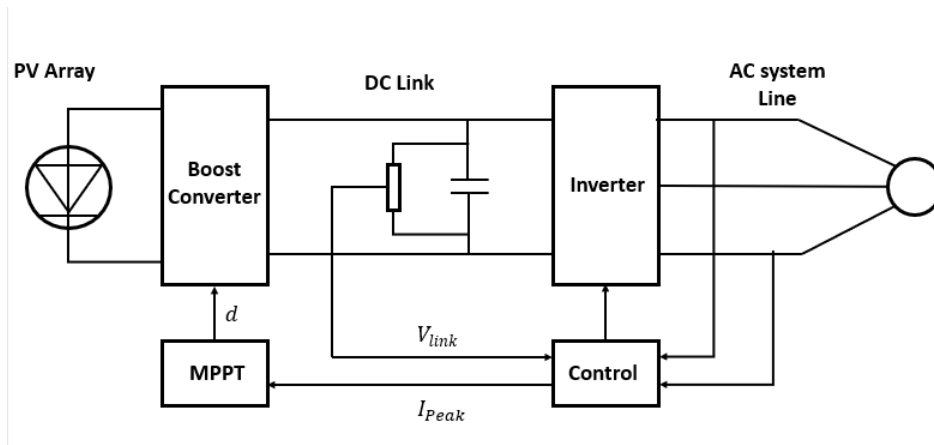


Figure 2.11 - Topology of a DC-Link Capacitor Droop Control

2.2.10 Load Current or Load Voltage Maximization

As previously stated, the maximization of the power coming from the PV array, will also maximize the power at the load of the converter. Using this train of thought, in reverse, the maximization of the output power at the load will amplify the PV array power. For most of the loads, the increase of the load current or load voltage will maximize the load power, making the necessity of only one sensor. Being that, a battery can be seen as a voltage-source type load, the load current can be used as the control variable.

This kind of MPPT [11][31] technique cannot operate continually at the MPP since the system revolves around the assumption of a lossless power converter.

2.2.11 dP/dV or dP/dI Feedback Control

With the availability of devices capable of performing complex computations such as microcontrollers and DSP, one easy way of performing the tracking of the MPP is through the slope of the PV power curve (dP/dV or dP/dI) and drive it back to the power converter pointing it to zero. This kind MPPT [11][32] is usually quite fast.

2.3 Comparison of MPPT methods

In Table 2.2 can be seen the characteristics of all the methods shown in this chapter. There are a wide variety of MPPT techniques with different properties. Most of the MPPT techniques can be used by almost all systems, but in some cases a MPPT technique may be more suitable over other, some of these causes may be because costs, the location of the system (easy accessibility, or constant variations in the environment), requirement of precision, energy available, among others.

The characteristics shown in the Table 2.2 can affect the function of the MPPT technique as some need to be flexible and able to operate in different types of PV arrays, a requirement of precision where in case of multiple MPP the true MPP is desired so that the maximum efficiency can be achieved, the scale of the project since periodic adjustments might not be a sensible solution.

In this thesis, since a low-power PV cell is used, a suitable MPPT controller must have low power consumption. As such low power computation complexity and low power components are preferred, as the benefits of the MPPT method might be mitigated by its power consumption. From the tracking methods represented in the Table 2.2 the P&O method and IncCond methods were selected to be implemented, since both methods show low to average complexity and the essential feature of low power consumption.

MPPT Technique	PV array dependency	True MPP	Analog or Digital	Periodic Calibration	Convergency Speed	Complexity	Required Parameters	Power Consumption
Hill-climbing/P&O	No	Yes	Both	No	Varies	Low	Voltage, Current	Low
IncCond	No	Yes	Digital	No	Varies	Average	Voltage, Current	Low
Fractional Voc	Yes	No	Both	Yes	Average	Low	Voltage	Low
Fractional Isc	Yes	No	Both	Yes	Average	Average	Current	Low
Fuzzy Logic Control	Yes	Yes	Digital	Yes	Fast	High	Varies	High
Neural Network	Yes	Yes	Digital	Yes	Fast	High	Varies	High
RCC	No	Yes	Analog	No	Fast	Low	Voltage, Current	Low
Current Sweep	Yes	Yes	Digital	Yes	Slow	High	Voltage, Current	High
DC Link Capacitor Droop Control	No	No	Both	No	Average	Low	Voltage	Low
Load I or V Maximization	No	No	Analog	No	Fast	Low	Voltage, Current	Low
dP/dV or dP/dI Feedback control	No	Yes	Digital	No	Fast	Average	Voltage, Current	High

Table 2.2 - Characteristics of various MPPT Technique

CHAPTER 3

PROPOSED SYSTEMS

As previously mentioned, the objective of this thesis is looking through the available MPPT techniques and find a couple that are reliable in an implementation of a low energy circuit. As such there will be selected two different MPPT methods, where these will increase the efficiency of a system where the energy will be received through a PV cell, raised through a DC-DC boost Converter as shown in Figure 3.1.

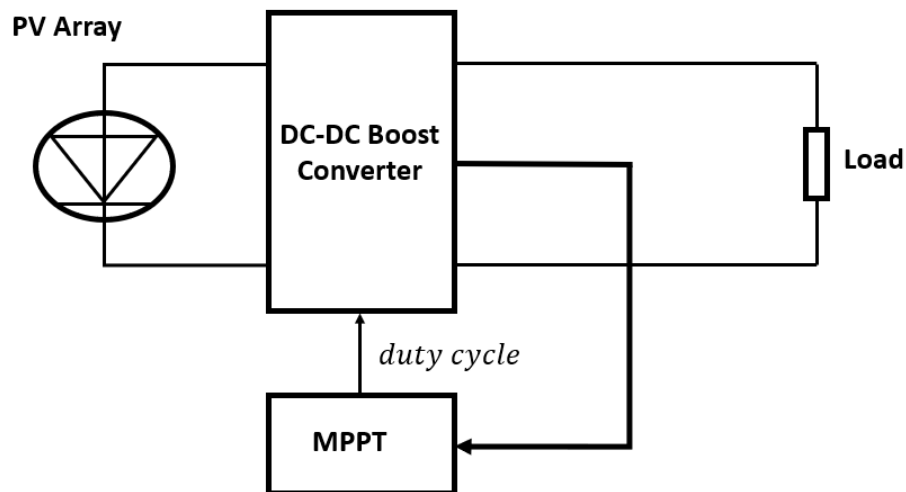


Figure 3.1 - Proposed MPPT algorithm for PV application

3.1 PV array

The PV cell was modelled from the model available in the MATLAB libraries, in which the characteristic parameters of the cell were adjusted, as represented by the table 3.1 (when irradiation is 1000 W/m^2 and the temperature is 25°C), so the PV cell can be similar to a generally used in this kind of project. The I-V and P-V curves can be seen in 3.2.

Voc (V)	Vmp (V)	Isc (mA)	Imp (mA)
1.5	1.3	4	3.8

Table 3.1 - PV cell parameters

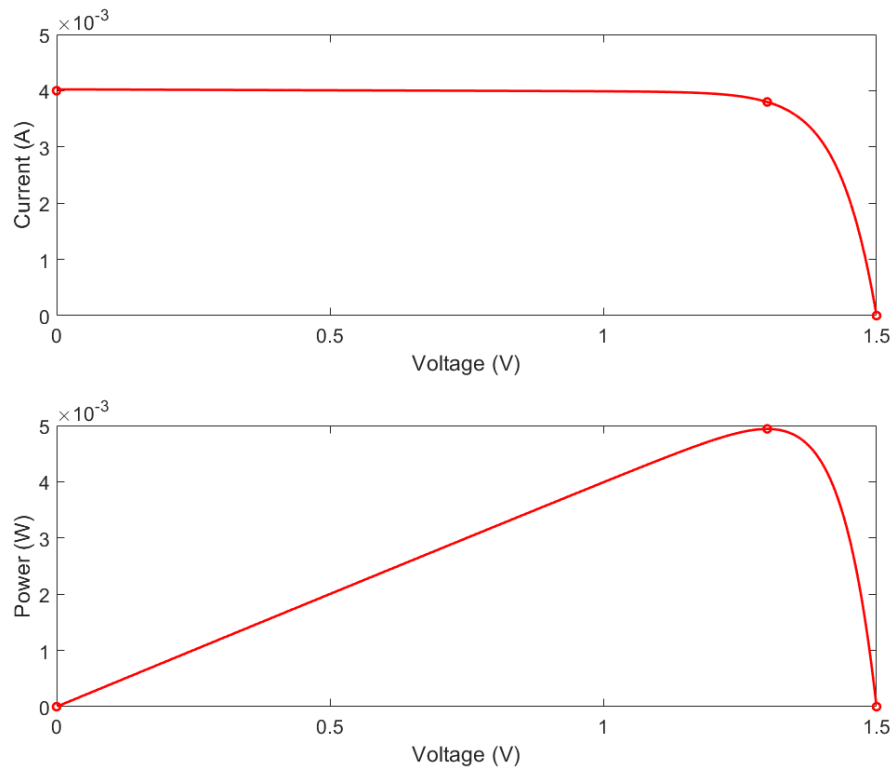


Figure 3.2 - PV cell IV and PV curves

In order to correctly simulate the behaviour of the MPPT's when the PV cell is subjected to changing environments, through the tests the values of irradiance and temperature are modified, these consequently alter the normal function of the PV cell. As represented by the figures 3.3 and 3.4 the effects caused by changes in radiation and temperature will have effects in the performance of the PV cell. The effectiveness is greatly impacted when lack of irradiation is available to the PV cell. In contrast, when the lower the temperature verified in the PV cell the better it will perform.

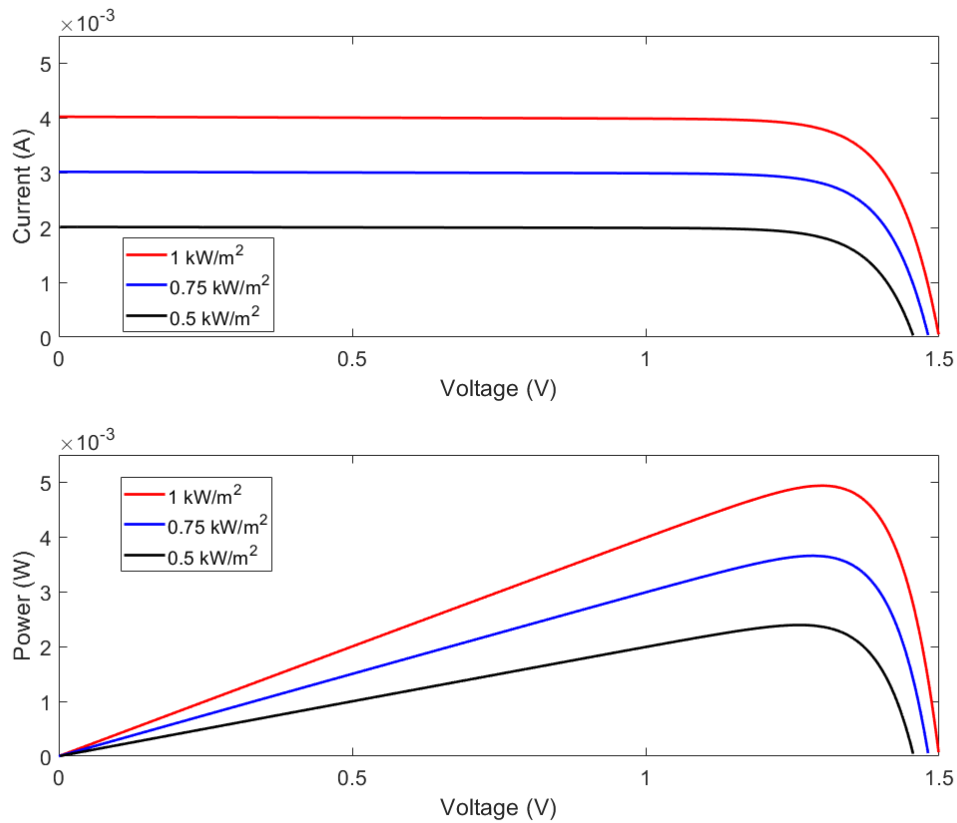


Figure 3.3 - Effect of different values of irradiance in a PV cell at 25°C

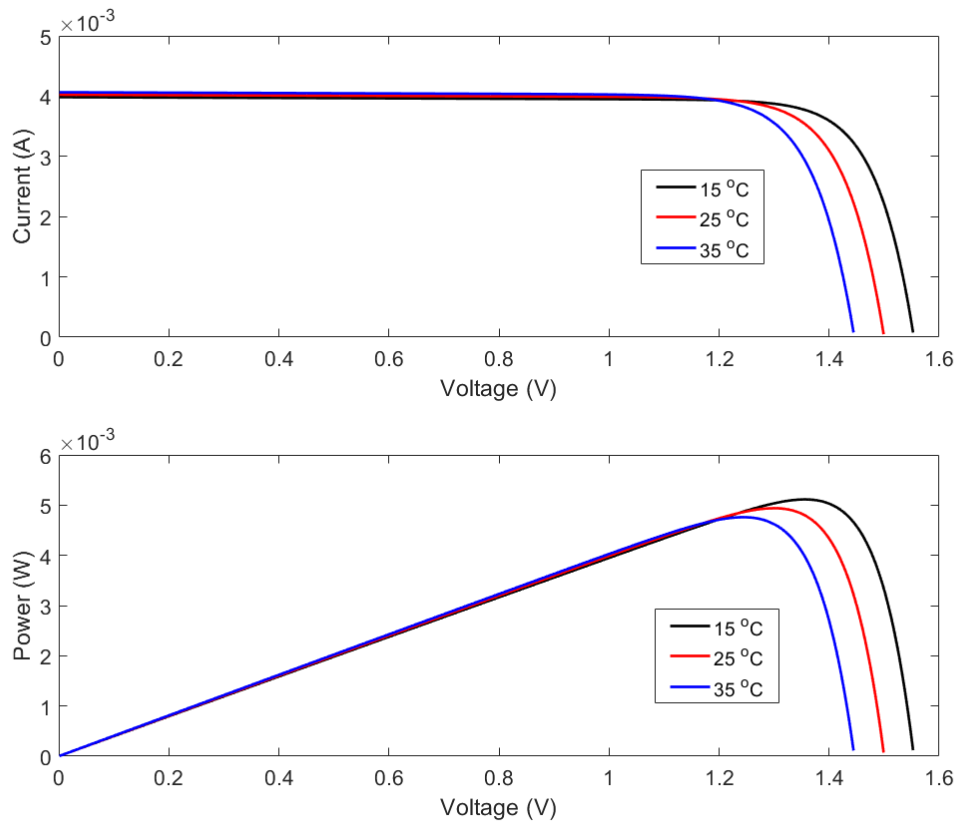


Figure 3.4 - Effect of Temperature variations in a PV cell at $1KW/m^2$

3.2 DC-DC boost Converter

The DC-DC converter selected will be a basic voltage converter (Figure 2.3) that will provide a step-up voltage to the load.

The DC-DC boost converter model developed for this thesis in the tool Simulink of MATLAB, is represented in the Figure 3.5.

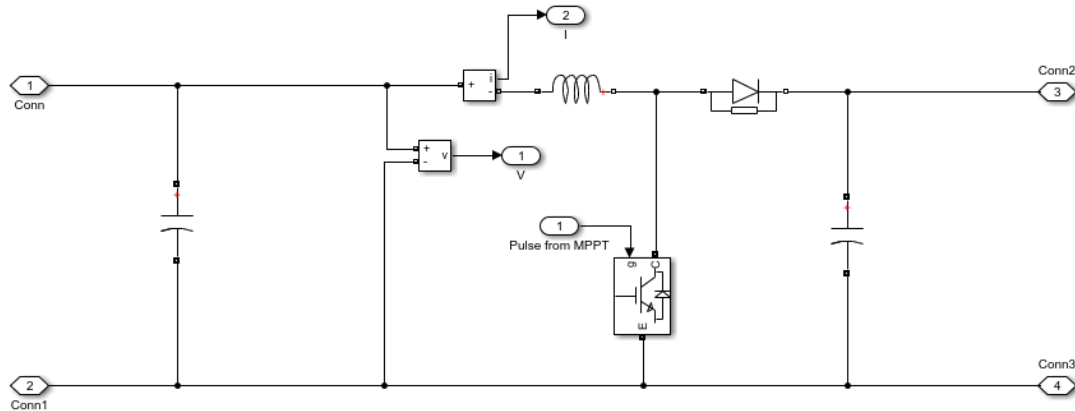


Figure 3.5 - Simulink model of DC-DC boost converter

The values to the inductor and capacitors can be obtained using the equations (2.1 - 2.10). Being that in this work it was used a frequency of 1MHz and as previously mentioned the PV array has 1.3 V_{mp} to get the highest possible voltage in the output of the DC-DC, the parameters needed for this converter can be seen in the table .

Frequency	1MHz
C_{out}	0.1 μF
L	151 μH / 150 μH *

Table 3.2 - Converter sizing *instead of the calculated 151uH the 150uH can be found in the market

In Figure 3.6 are represented the pulses and voltages in the switch of the boost DC-DC converter as well as the current in the inductor.

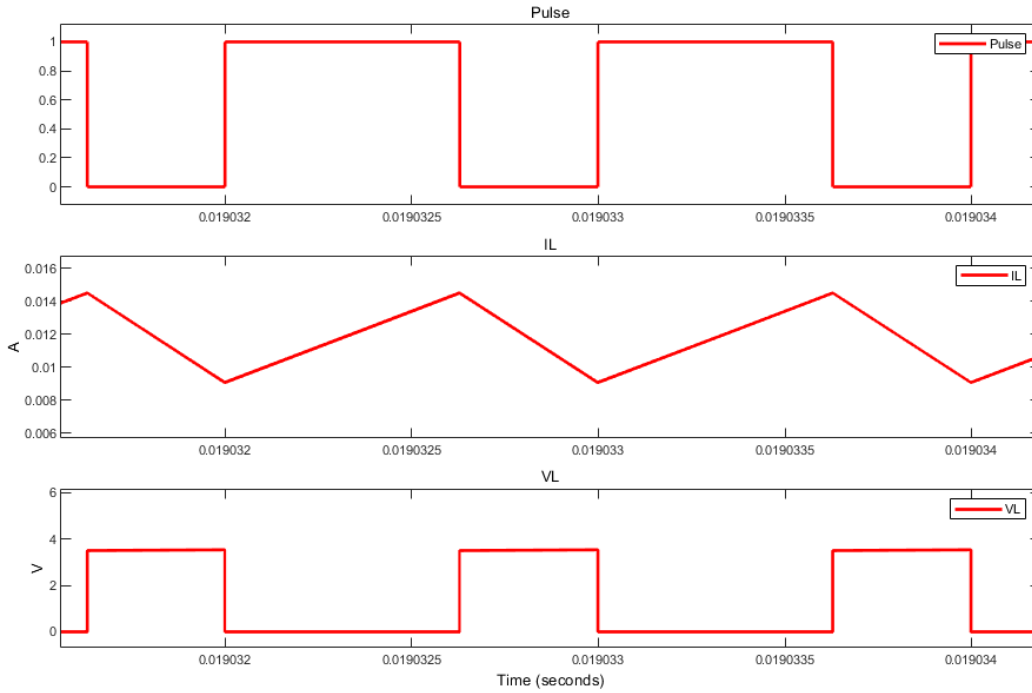


Figure 3.6 - Pulses and voltage of the switch and inductor current

3.3 Max power point tracking method

As a PV cell is used as the source of power for this project, fluctuations in its temperature and irradiation will impact the functioning of a PV cell. Consequently, the value of duty cycle must be able to adapt itself so that the system keeps functioning at its MPP, therefore the system should be able to adjust its duty cycle.

The models are constituted by two sections, the MPPT that will control the changes of the duty cycle in the PWM, where the frequency of work will be set, that will generate the signal of the duty cycle to be used as reference for the switch of the boost DC-DC as it can be seen in 3.5 and 3.6.

The system is represented in the figure 3.7, where is constituted by three main blocks the PV array, the boost DC-DC and the MPPT.

The main variables are the irradiation, temperature, and frequency. The irradiation and temperature can be modified to simulate any type of combinations between these two variables in a signal builder as it can be seen in 3.7.

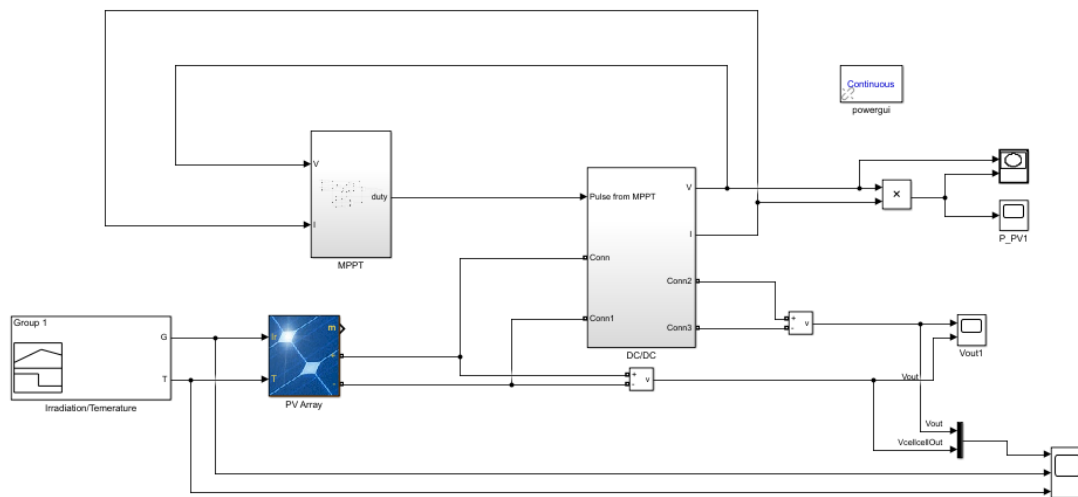


Figure 3.7 - MPPT PV cell powered system

3.3.1 Perturb and observe

The P&O MPPT technique model can be designed in SIMULINK as in figure 3.8.

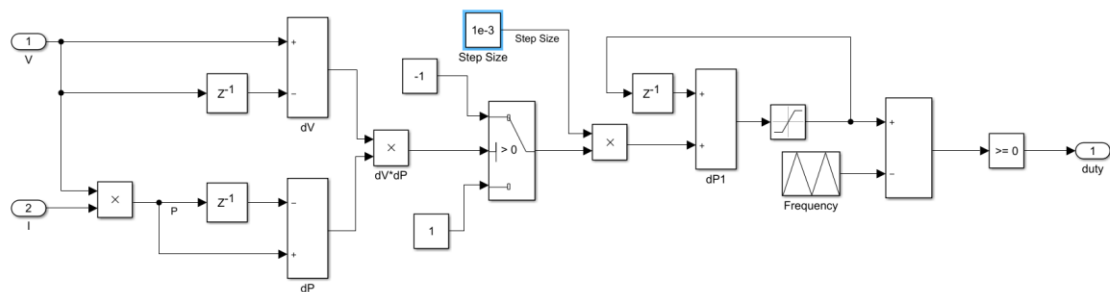


Figure 3.8 - Model of P&O

Shown in the Figure 2.9 is the model will take the Voltage and Current from the PV cell this way the system is able to balance itself in the MPP as previously stated, the step size of the perturbances can be adjusted in the highlighted variable making possible the control of precision and convergence speed.

3.3.2 Incremental Conductance Max power point tracking method

Model of the Incremental Conductance in SIMULINK as in figure 3.9.

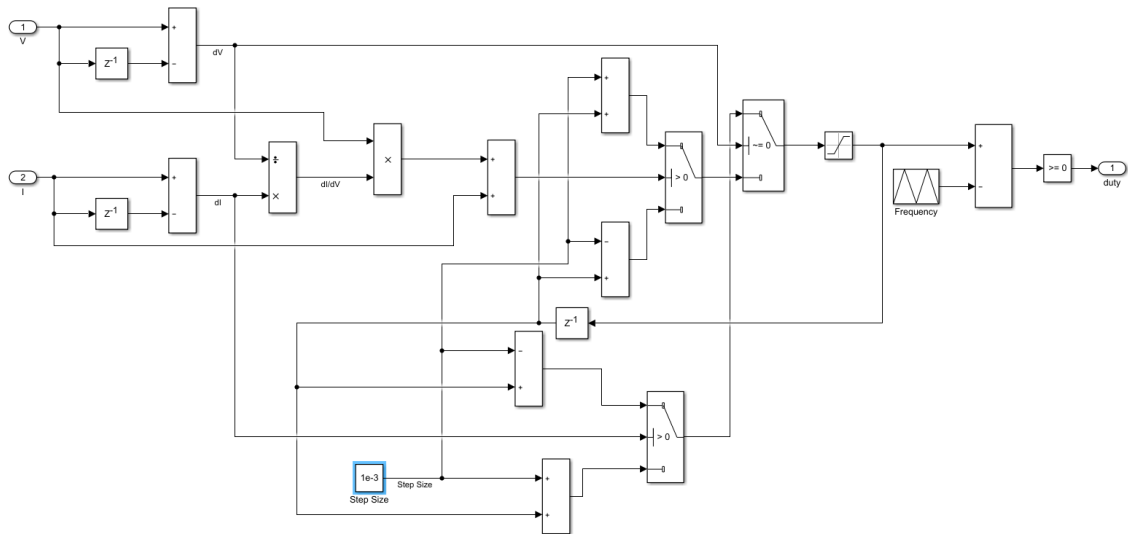


Figure 3.9 - Model of IncCond

Shown in the Figure 2.10 is the model will take the Voltage and Current from the PV cell this way the system is able to self-sustained the MPP as previously stated, once again in the highlighted variable will control convergence speed and precision of the MPPT.

CHAPTER 4

SIMULATIONS AND RESULTS

In this chapter the results and simulations of the proposed systems will be shown. To keep in mind that the simulations are focused in the changes of irradiance and temperature, leaving negligible the parasitic effects, as well as, all the simulations were executed using the SIMULINK tool from MALTAB.

To make comparison of the results accurate, all the tests will occur under the same conditions of temperature and irradiation as shown in the Fig. 4.1.

In order to observe the impact of the use of a MPPT technique in this kind of systems another system will be used in comparison, where no MPPT method is used and will function by applying a fixed duty cycle to the switch in the DC-DC converter.

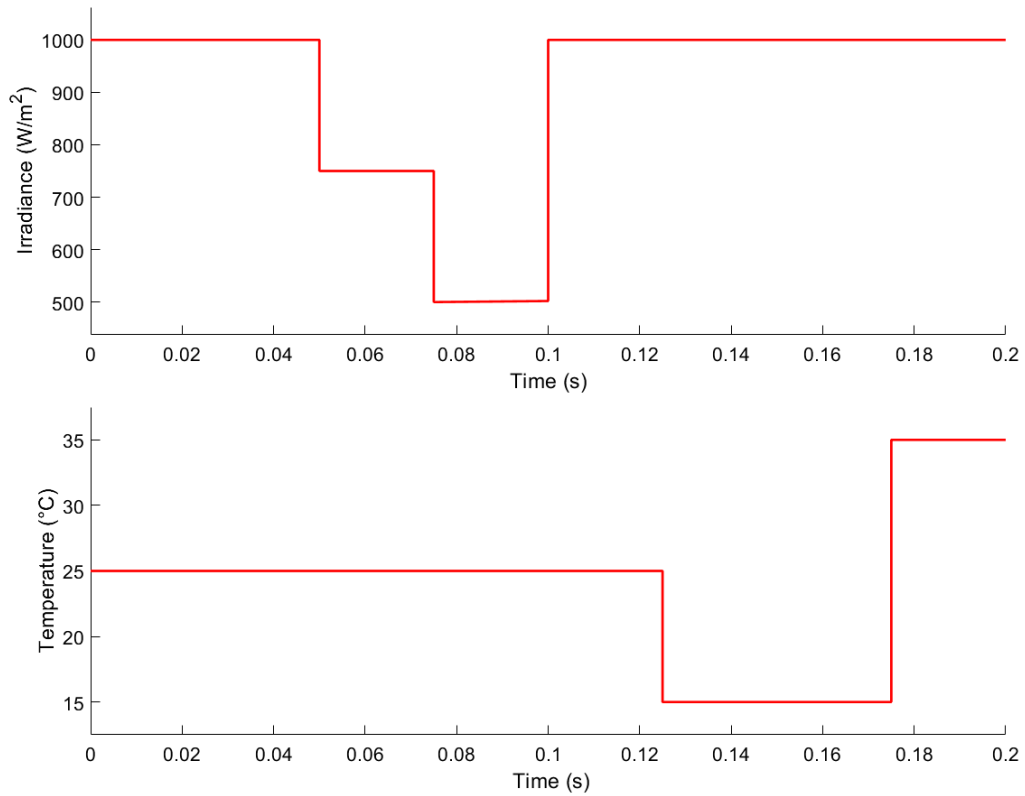


Figure 4.1 - Irradiance and Temperature changes in the simulations

All tests will occur during the same 0.2 seconds, where in the first 0.1 seconds the changes in irradiation will be applied and in the remainder of the time the variations in temperature. The values of irradiation chosen are $1000W/m^2$, $750W/m^2$ and $500W/m^2$, as for testing the impact of temperature the values chosen where $35^{\circ}C$, $25^{\circ}C$ and $15^{\circ}C$. Each one of these values will run within a time frame where the system is able to adjust to these new parameters.

<i>Time (s)</i>	0 – 0.05	0.05 – 0.075	0.075 – 0.1
<i>Irradiance (W/m²)</i>	1000	750	500
<i>Power (* 10⁻³W)</i>	4.94	3.659	2.395

Table 4.1 - MPP of the PV cell with varying the irradiance

<i>Time (s)</i>	0.1 – 0.125	0.125 – 0.175	0.175 – 0.2
<i>Temperature(°C)</i>	25	15	35
<i>Power (* 10⁻³W)</i>	4.94	5.114	4.76

Table 4.2 - MPP of the PV cell with varying the temperatures

Represented in the Tables 4.1 and 4.2 are the values of the true MPP of the PV cell in each condition of irradiation and temperature change. These values can be used to evaluate the effectiveness of each method used.

4.1 Simulations of the DC-DC Converters

4.1.1 Without a MPPT technique

To use a fixed duty cycle in the project, a pulse generator is used to control the switch of the boost DC-DC, as represented by the Figure 4.2. The pulse generator was set to perform at 1MHz and the value of 58% for the duty cycle as this value is the one that enables the best performance of the system, under the conditions of Irradiation $1000\text{W}/\text{m}^2$ and cell temperature $25\text{ }^\circ\text{C}$.

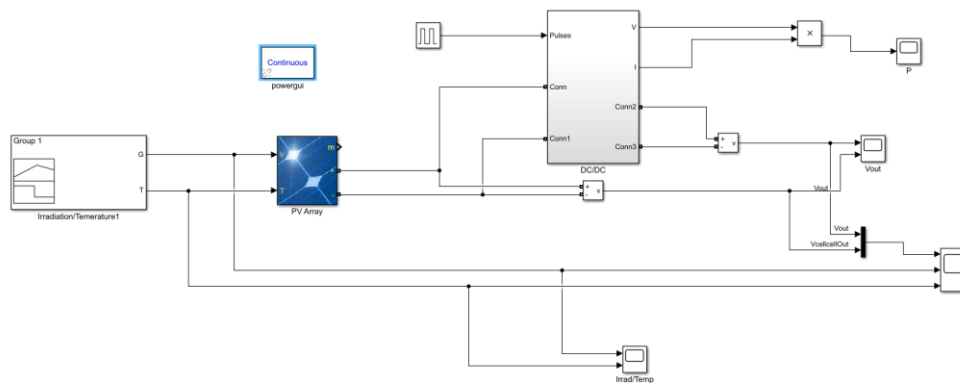


Figure 4.2 - System without MPPT technique

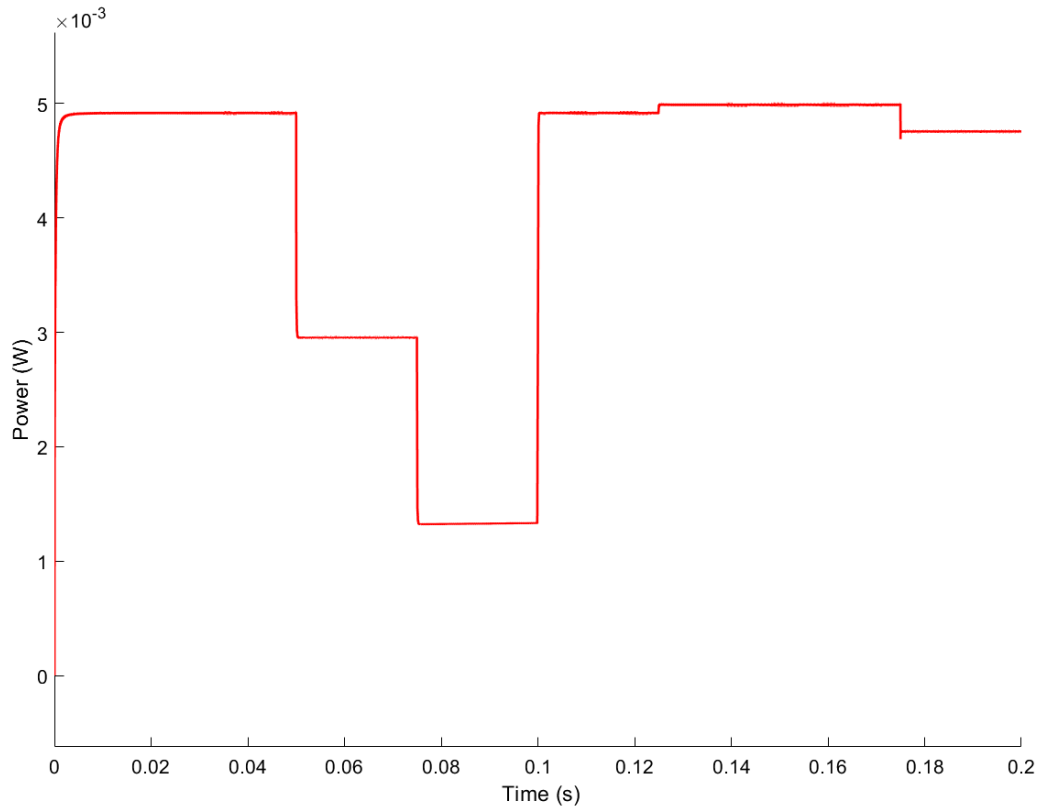


Figure 4.3 - PV cell Power without MPPT

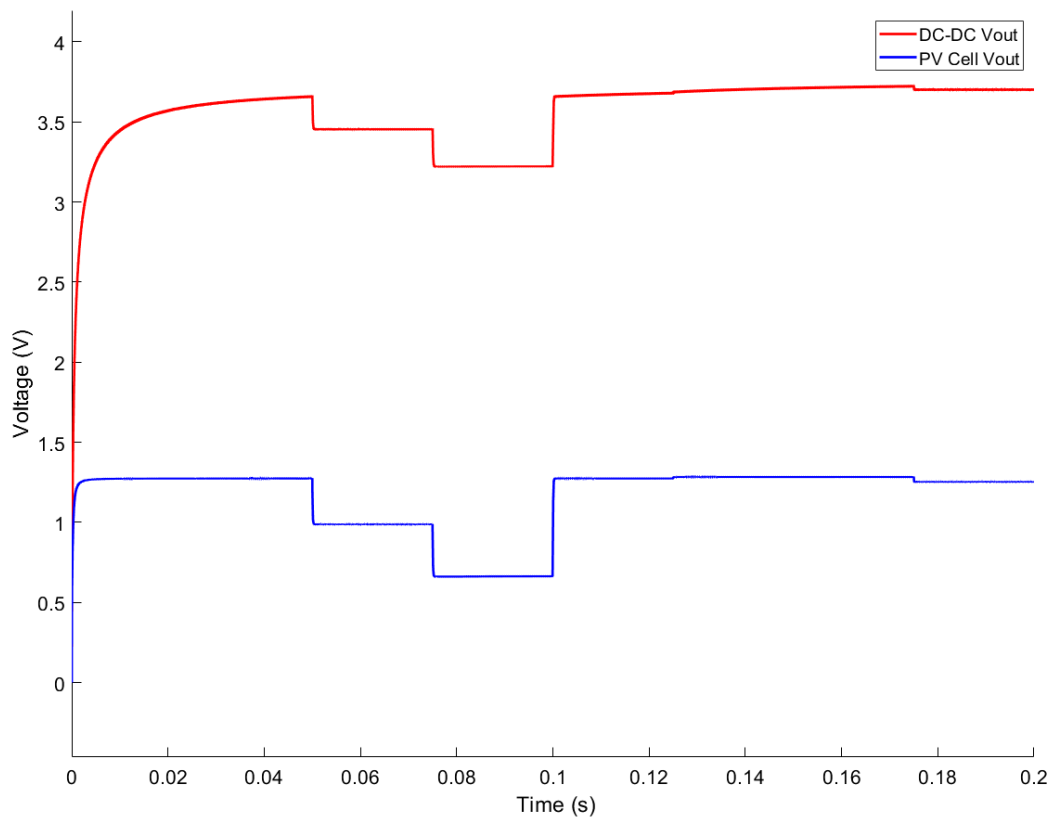


Figure 4.4 - PV cell voltage and DC-DC output voltage

<i>Time (s)</i>	0 – 0.05	0.05 – 0.075	0.075 – 0.1
<i>Irradiance (W/m²)</i>	1000	750	500
<i>Power (* 10⁻³W)</i>	4.918	2.954	1.322
<i>PV Voltage (V)</i>	1.274	0.987	0.661
<i>DC – DC Vout (V)</i>	3.658	3.454	3.22
<i>η (%)</i>	99.55	80.73	55.19

Table 4.3 - Circuit with no MPPT with varying the irradiance

<i>Time (s)</i>	0.1 – 0.125	0.125 – 0.175	0.175 – 0.2
<i>Temperature(°C)</i>	25	15	35
<i>Power (* 10⁻³W)</i>	4.918	4.99	4.756
<i>PV Voltage (V)</i>	1.274	1.283	1.253
<i>DC – DC Vout (V)</i>	3.68	3.722	3.702
<i>η (%)</i>	99.55	97.57	99.91

Table 4.4 - Circuit with no MPPT with varying temperature

Represented by the Figures and Tables 4.3 and 4.4 are the simulations where no MPPT technique is present. It can be examined that the performance of the system drops exponentially the further away the cell is from its starting conditions. When PV cell operates near these initial conditions the system shows efficiencies from 99.55% to 97%, in contrast when the PV cell performs with 500 W/m² the efficiency is as low as 55%.

4.1.2 With P&O

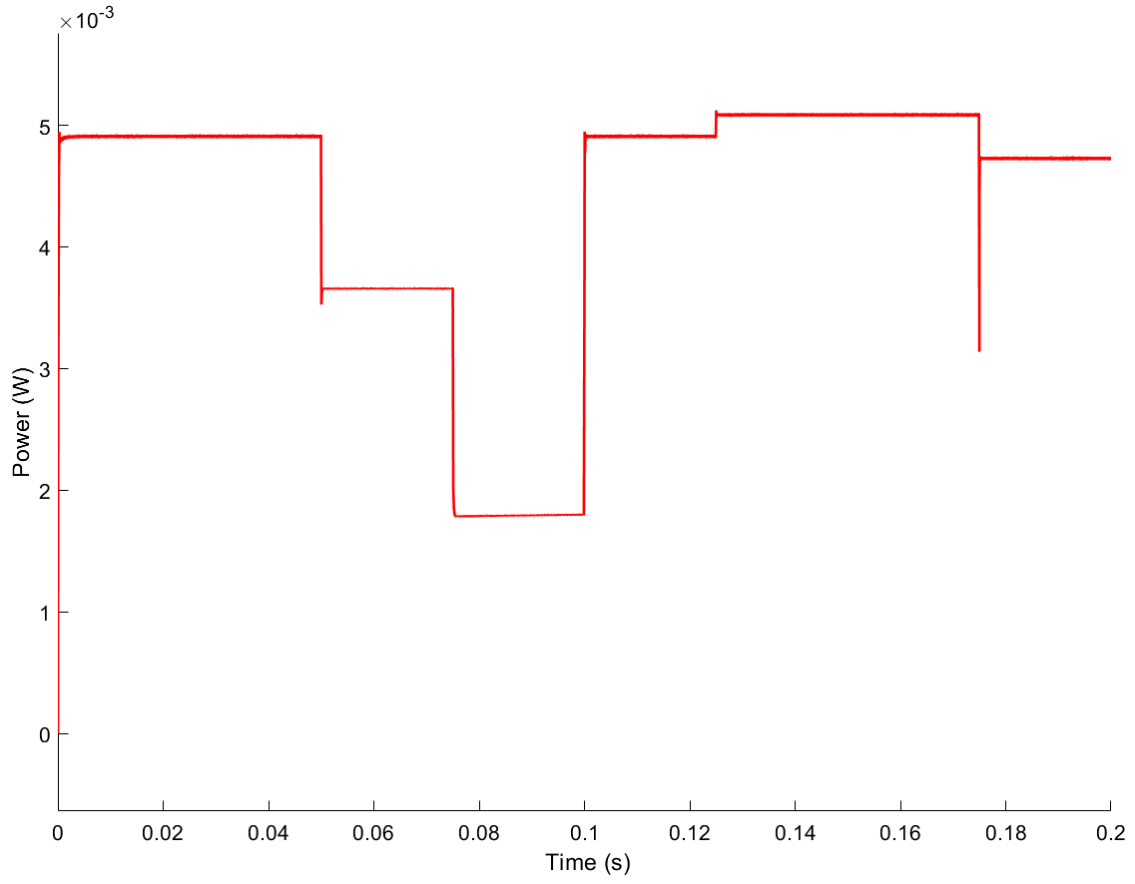


Figure 4.5 - PV cell Power with P&O MPPT

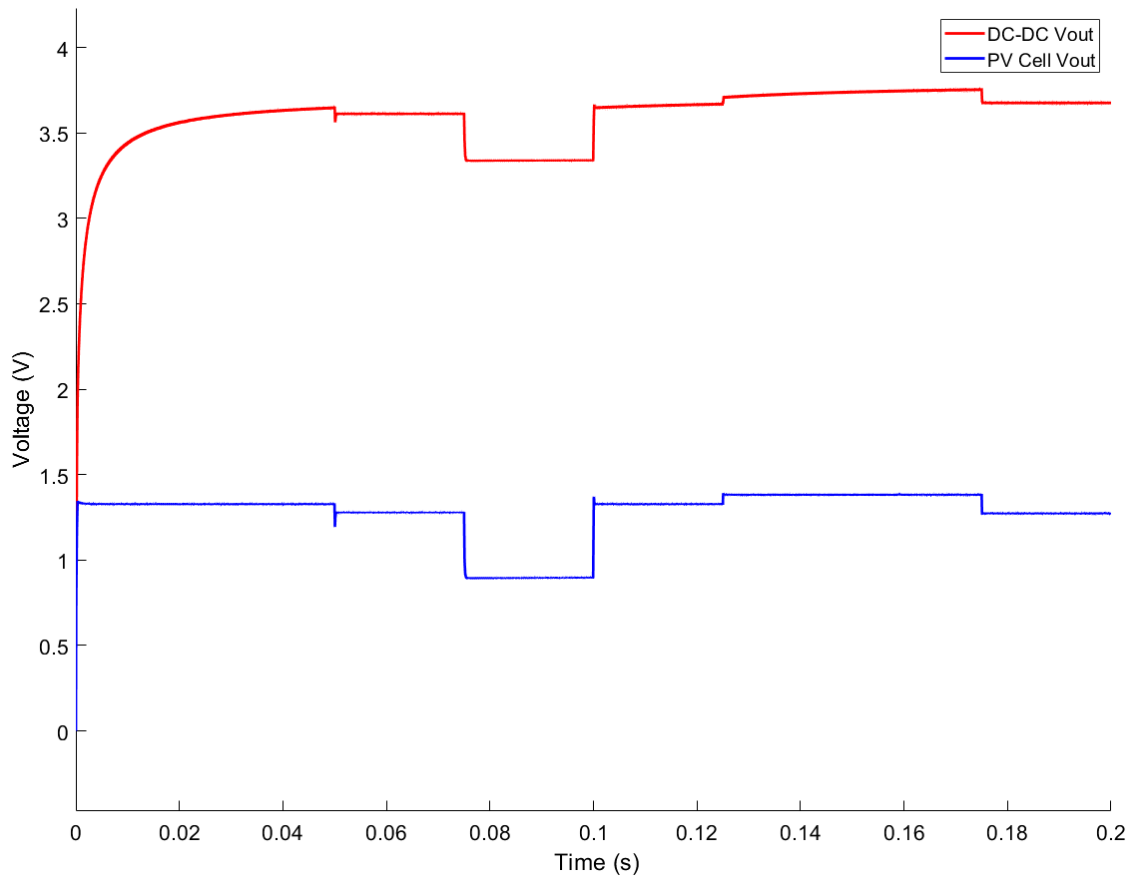


Figure 4.6 - PV cell voltage and DC-DC output voltage with P&O

Time (s)	0 – 0.05	0.05 – 0.075	0.075 – 0.1
Irradiance (W/m^2)	1000	750	500
Power ($* 10^{-3}W$)	4.91	3.658	1.799
PV Voltage (V)	1.328	1.279	0.894
DC – DC Vout (V)	3.65	3.616	3.34
$\Delta\eta(\%)*$	-1.63	23.83	36.08
$\eta(\%)$	99.39	99.97	75.11

Table 4.5 - Circuit with P&O with varying irradiance

<i>Time (s)</i>	0.1 – 0.125	0.125 – 0.175	0.175 – 0.2
<i>Temperature(°C)</i>	25	15	35
<i>Power (* 10⁻³W)</i>	4.91	5.087	4.727
<i>PV Voltage (V)</i>	1.327	1.382	1.273
<i>DC – DC Vout (V)</i>	3.67	3.754	3.676
<i>Δη(%)*</i>	-1.63	1.943	-0.609
<i>η (%)</i>	99.39	99.47	99.30

Table 4.6 - Circuit with P&O with varying temperature

The Figures and Tables 4.5 and 4.6 shows the results of the simulations using the P&O technique, observing Figure 4.5 and comparing it to the 4.3 it can be observed oscillations, as these represent the MPPT control adjustments, as it maintains the PV cell at MPP. While using P&O, the effects of the environment have less impact to the system, than the previous test, as at an irradiation of 500 W/m² the efficiency is still upwards of 75%. While comparing the η to the previous model there are improvements from 23% – 36%. Comparing to the work in [33] results were similar since, the P&O method is used in a low power system, in which tests were performed under varying weather conditions, from sunny days without shading conditions to cloudy weather, these tests showed the P&O efficiency decay from 95.9% in sunny weather to 75.5% when the tests where realised under cloudy conditions.

4.1.3 With Incremental Conductance

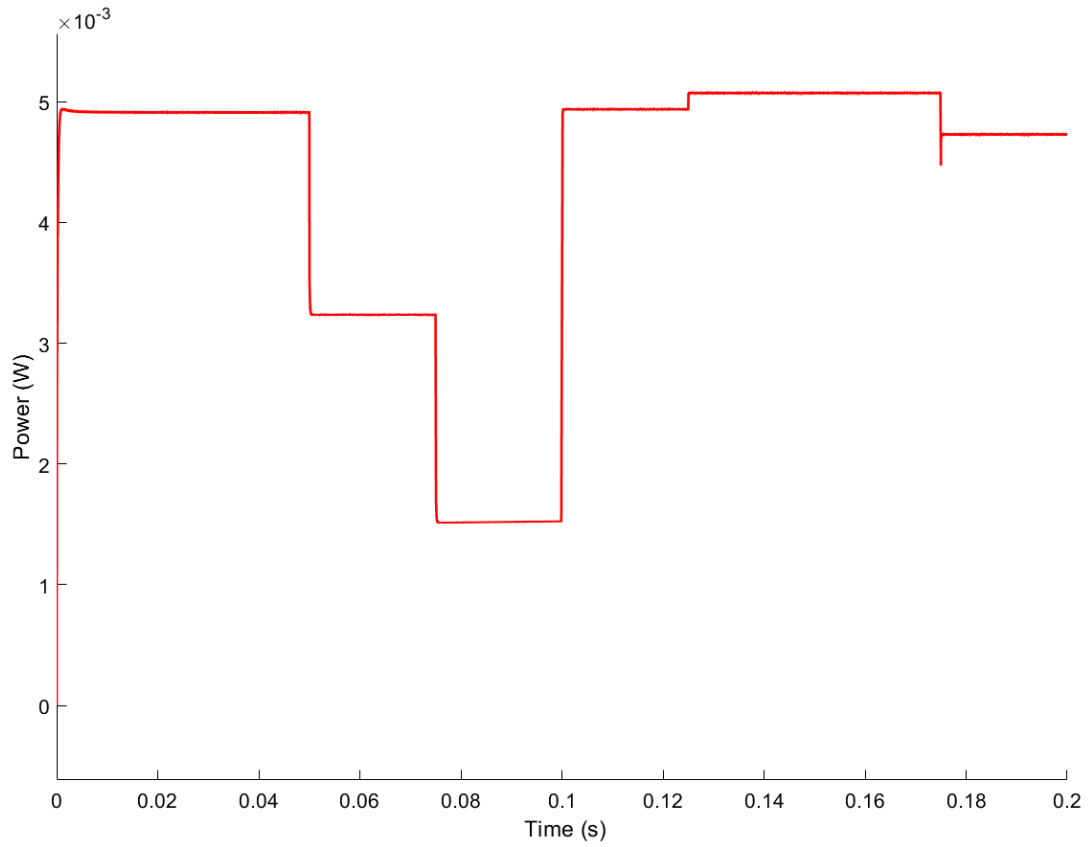


Figure 4.7 - PV cell Power with IncCond MPPT

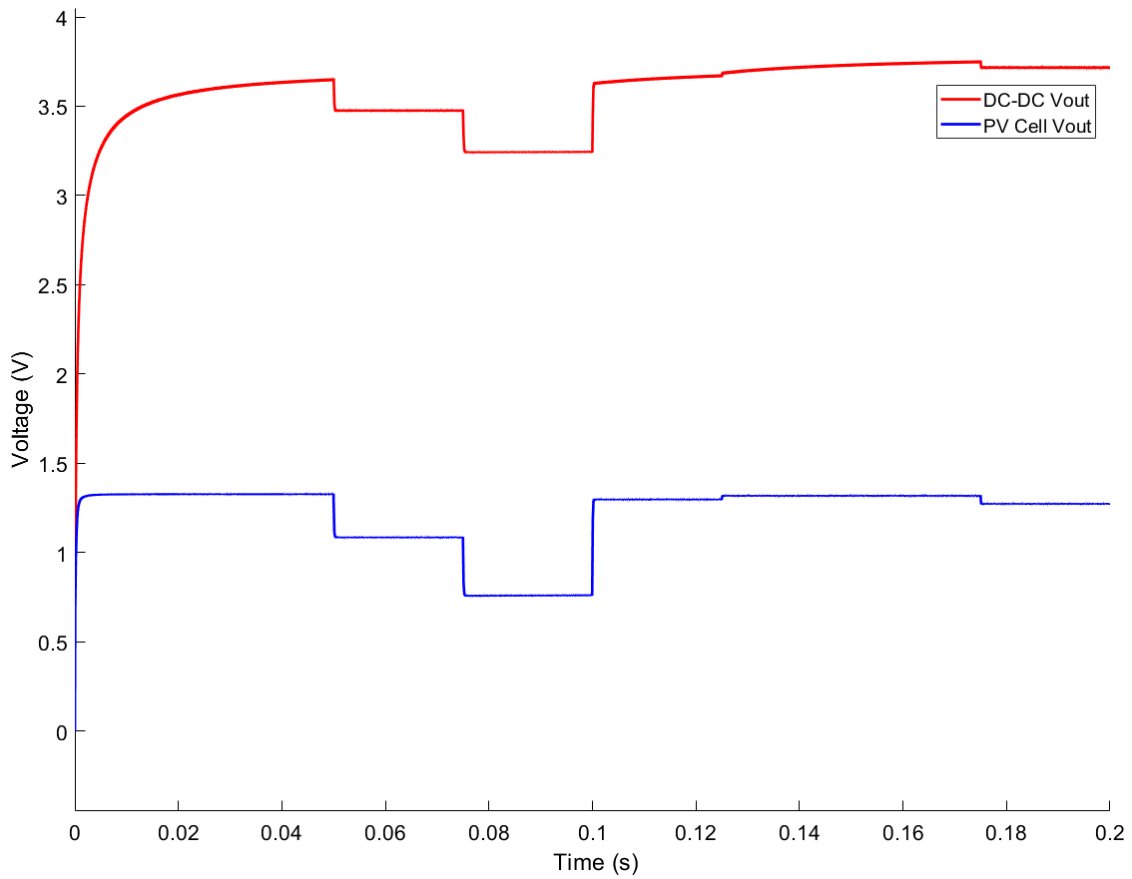


Figure 4.8 - PV cell voltage and DC-DC output voltage with IncC

<i>Time (s)</i>	0 – 0.05	0.05 – 0.075	0.075 – 0.1
<i>Irradiance (W/m²)</i>	1000	750	500
<i>Power (* 10⁻³W)</i>	4.919	3.223	1.506
<i>PV Voltage (V)</i>	1.324	1.079	0.754
<i>DC – DC Vout (V)</i>	3.651	3.476	3.243
<i>Δη(%)*</i>	0.02	9.11	13.92
<i>η (%)</i>	99.57	88.04	62.88

Table 4.7 - Circuit with IncCond with varying irradiance

<i>Time (s)</i>	0.1 – 0.125	0.125 – 0.175	0.175 – 0.2
<i>Temperature(°C)</i>	25	15	35
<i>Power (* 10⁻³W)</i>	4.936	5.065	4.735
<i>PV Voltage (V)</i>	1.293	1.313	1.27
<i>DC – DC Vout (V)</i>	3.67	3.756	3.715
<i>Δη(%)*</i>	0.366	1.503	-0.442
<i>η (%)</i>	99.91	99.04	99.47

Table 4.8 - Circuit with IncCond with varying temperature

In the Figures and Tables 4.7 and 4.8 are represented the results of the simulations using the IncCond method. As the previous method, using a MPPT will retard the effects of the environment, maintaining the system reliable while changes in the environment occur. With the IncCond, the values of η in the tests vary from 99% – 62%. While comparing the results of this technique with the first tested, improvements from 9% – 13% can be verified.

* $\Delta\eta$ between the models with MPPT techniques and the one not using any

4.2 Discussion

Comparing all the results, is analysed that there are some vantages and disadvantages in every method.

Tests where no MPPT method was present, performs better in the ideal conditions of the PV cell, otherwise when the parameters of irradiation and temperature diverge from the initial values, the performance starts to drop exponentially, and other methods start to outperform the direct duty-cycle method. In contrast, the most reliable method when the further away the initial conditions are verified, is the P&O implementation as represented by the tables, when an irradiance of $500W/m^2$ is verified, the efficiency is 75.11%, in comparison the IncCond technique when performing under the same conditions can only obtain efficiency of 62.88%. Finally, the IncCond is an intermediate of both techniques mentioned previously, as when near initial irradiation and temperature conditions outperform the P&O technique and shows better performance than the process with no MPPT when changes in the environment affect the PV cell. Therefore, in cases when it is guaranteed that the cell will only operate in favourable and low varying environments the selection of the IncCond method is the more appropriated, as it

has been previously mentioned. Otherwise, in cases where there are constant variations in irradiation available, the most suitable is the P&O method, as it is the most reliable under varying conditions.

CHAPTER 5

CONCLUSIONS AND FUTURE WORK

5.1 Conclusions

The main goal of this work is to look and compare the implementation of Maximum Power Point Tracking techniques into a PMU that can boost the input voltage. Since this PMU resorts to the harvest photovoltaic energy, the system is required to operate at the max power point of the PV cell.

Two different MPPT control methods for a DC-DC converter were developed in this thesis, both MPPT's perform desirably as exhibited in chapter 4, either one of them is capable to adapt to the environment. Benefits from these are amplified the further the PV cell is to perform away from its peak.

Moreover, both methods are suited to small portable devices with low energy. However, both methods can fall short in some cases as these don't operate in the true MPP, since the compromise to obtain the true MPP would consume additional energy by the MPPT method controller.

Regarding performance, both methods show differences, where the P&O method performs better the further away the conditions for the operation of the PV system, when performing under the irradiation of $500W/m^2$ it exhibits 75.11% of efficiency, on the other and the Incremental conductance MPPT performs at 62.88%. In contrast, the Incremental conductance method performs better when the environment is favourable for the PV cell performance.

Furthermore, the results in this thesis can be compared with the results in work [33], where the efficiency of P&O vary from 99.5% – 75.5%.

5.2 Future Work

For future work, the models developed in this thesis can be imported, compiled, and implemented through Verilog HDL, and CMOS so that physical tests can be performed enabling comparison with the model results.

Furthermore, the substitution of the generic photovoltaic cell used with the PV cells recently developed in FCT-UNL, since these are lighter and flexible.

In addition, the use of a different energy harvesting technique, or implementing a different MPPT method could be tested.

BIBLIOGRAPHY

- [1] "Number of network connected devices per person around the world from 2003 to 2020" statista 2015 URL: <https://www.statista.com/statistics/678739/forecast-on-connected-devices-per-person/>.
- [2] T.Ruan, Z.Chew and M.Zhu. "Energy-aware Approaches for Energy Harvesting Powered Wireless Sensor Nodes" In: IEEE Sensors Journal 17.7 , pp. 2165-2173. doi:10.1109/jsen.2017.2665680, 2017.
- [3] C. Alippi, and C. Galperti, "An adaptive system for optimal solar energy harvesting in wireless sensor network nodes," IEEE Trans. Circuits Syst. I, Reg. Papers, vol. 55, no. 6, pp. 1742-1750, 2008.
- [4] W. Wang, V. Cionca, N. Wang, M. Hayes, B. O'Flynn, and C. O'Mathuna, "Thermoelectric energy harvesting for building energy management wireless sensor networks," Int. J. Distrib. Sens.Netw., vol. 2013, pp. 14, 2013.
- [5] N. Kong, and D.-S. Ha, "Low-power design of a self-powered piezoelectric energy harvesting system with maximum power point tracking," IEEE Trans. Power Electron., vol. 27, no. 5, pp. 2298-2308, 2012.
- [6] Y. K. Tan, and S. K. Panda, "Optimized wind energy harvesting system using resistance emulator and active rectifier for wireless sensor nodes," IEEE Trans. Power Electron., vol. 26, no. 1, pp. 38-50, 2011.
- [7] T. Eswam, and P. L. Chapman, "Comparison of Photovoltaic Array Maximum Power Point Tracking Techniques", IEEE Trans. on energy conversion, vol. 22, no. 2, 2007.
- [8] L. L. Buciarelli, B. L. Grossman, E. F. Lyon, and N. E. Rasmussen, "The energy balance associated with the use of a MPPT in a 100 kW peak power system," in IEEE Photovoltaic Spec. Conf., pp. 523-527, 1980.
- [9] J. D. van Wyk and J. H. R. Enslin, "A study of wind power converter with microprocessor based power control utilizing an oversynchronous electronic scherbius cascade," in Proc. IEEE Int. Power Electron. Conf., pp. 766-777, 1983.
- [10] W. J. A. Teulings, J. C. Marpinard, A. Capel, and D. O'Sullivan, "A new maximum power point tracking system," in Proc. 24th Annu. IEEE Power Electron. Spec. Conf., pp. 833-838, 1993.

- [11] T. Eswam, and P. L. Chapman “Comparison of Photovoltaic Array Maximum Power Point Tracking Techniques” IEEE TRANSACTIONS ON ENERGY CONVERSION, VOL. 22, NO. 2, 2007.
- [12] O. Wasynczuk, “Dynamic behaviour of a class of photovoltaic power systems,” IEEE Trans. Power App. Syst., vol. 102, no. 9, pp. 3031–3037, 1983.
- [13] M. A. Slonim and L. M. Rahovich, “Maximum power point regulator for 4 kW solar cell array connected through inverter to the AC grid,” in Proc. 31st Intersociety Energy Conver. Eng. Conf., 1996, pp. 1669–1672, 1996.
- [14] K. H. Hussein and I. Mota, “Maximum photovoltaic power tracking: An algorithm for rapidly changing atmospheric conditions,” in IEE Proc. Generation Transmiss. Distrib., 1995, pp. 59–64, 1995.
- [15] T.-Y. Kim, H.-G. Ahn, S. K. Park, and Y.-K. Lee, “A novel maximum power point tracking control for photovoltaic power system under rapidly changing solar radiation,” in IEEE Int. Symp. Ind. Electron., 2001, pp. 1011–1014, 2001.
- [16] Y.-C. Kuo, T.-J. Liang, and J.-F. Chen, “Novel maximum-power-point tracking controller for photovoltaic energy conversion system,” IEEE Trans. Ind. Electron., vol. 48, no. 3, pp. 594–601, 2001.
- [17] W. Wu, N. Pongratananukul, W. Qiu, K. Rustom, T. Kasparis, and I. Batarseh, “DSP-based multiple peak power tracking for expandable power system,” in Eighteenth Annu. IEEE Appl. Power Electron. Conf. Expo., pp. 525–530, 2003.
- [18] J. J. Schoeman and J. D. vanWyk, “A simplified maximal power controller for terrestrial photovoltaic panel arrays,” in Proc. 13th Annu. IEEE Power Electron. Spec. Conf., pp. 361–367, 1982.
- [19] D. J. Patterson, “Electrical system design for a solar powered vehicle,” in Proc. 21st Annu. IEEE Power Electron. Spec. Conf., pp. 618–622, 1990.
- [20] B. Bekker and H. J. Beukes, “Finding an optimal PV panel maximum power point tracking method,” in Proc. 7th AFRICON Conf. Africa, pp. 1125–1129, 2004.
- [21] T. Noguchi, S. Togashi, and R. Nakamoto, “Short-current pulse based adaptive maximum-power-point tracking for photovoltaic power generation system,” in Proc. 2000 IEEE Int. Symp. Ind. Electron., pp. 157–162, 2000.
- [22] N. Mutoh, T. Matuo, K. Okada, and M. Sakai, “Prediction-data-based maximum-power-point-tracking method for photovoltaic power generation systems,” in Proc. 33rd Annu. IEEE Power Electron. Spec. Conf., pp. 1489–1494, 2002.
- [23] M. Veerachary, T. Senjyu, and K. Uezato, “Neural-network-based maximum-power-point tracking of coupled-inductor interleaved-boost converter- supplied

- PV system using fuzzy controller,” *IEEE Trans. Ind. Electron.*, vol. 50, no. 4, pp. 749–758, 2003.
- [24] N. Khaehintung, K. Pramotung, B. Tuvirat, and P. Sirisuk, “RISCmicrocontroller built-in fuzzy logic controller of maximum power point tracking for solar-powered light-flasher applications,” in *Proc. 30th Annu. Conf. IEEE Ind. Electron. Soc.*, pp. 2673–2678, 2004.
- [25] R. M. Hilloowala and A. M. Sharaf, “A rule-based fuzzy logic controller for a PWM inverter in photo-voltaic energy conversion scheme,” in *Proc. IEEE Ind. Appl. Soc. Annu. Meet.*, pp. 762–769, 1992.
- [26] T. Hiyama, S. Kouzuma, and T. Imakubo, “Identification of optimal operating point of PV modules using neural network for real time maximum power tracking control,” *IEEE Trans. Energy Convers.*, vol. 10, no. 2, pp. 360–367, 1995.
- [27] K. Ro and S. Rahman, “Two-loop controller for maximizing performance of a grid-connected photovoltaic-fuel cell hybrid power plant,” *IEEE Trans. Energy Convers.*, vol. 13, no. 3, pp. 276–281, 1998.
- [28] P. Midya, P. T. Krein, R. J. Turnbull, R. Reppa, and J. Kimball, “Dynamic maximum power point tracker for photovoltaic applications,” in *Proc. 27th Annu. IEEE Power Electron. Spec. Conf.*, pp. 1710–1716, 1996.
- [29] M. Bodur and M. Ermis, “Maximum power point tracking for low power photovoltaic solar panels,” in *Proc. 7th Mediterranean Electrotechnical Conf.*, pp. 758–761, 1994.
- [30] T. Kitano, M. Matsui, and D.-h. Xu, “Power sensor-less MPPT control scheme utilizing power balance at DC link-system design to ensure stability and response,” in *Proc. 27th Annu. Conf. IEEE Ind. Electron. Soc.*, pp. 1309–1314, 2001.
- [31] E. E. Landsman, *Maximum Power Point Tracker for Photovoltaic Arrays*. Boston, MA: Massachusetts Institute of Technology Lincoln Labs, 1978.
- [32] R. Bhide and S. R. Bhat, “Modular power conditioning unit for photovoltaic applications,” in *Proc. 23rd Annu. IEEE Power Electron. Spec. Conf.*, pp. 708–713, 1992.
- [33] Veligorskyi, O. and Vagapov, Y. “Improvement of perturb and observe MPPT method for photovoltaic systems”: Case of study. *International Journal of Renewable Energy Technology*, Vol. 4, No. 2, pp. 141-156, 2013.
- [34] Carvalho, C “CMOS indoor light energy harvesting system for wireless sensing applications”, Doctoral dissertation, FCT/UNL, Portugal, 2014.